

This is a repository copy of *Identification of high performance solvents for the sustainable processing of graphene*.

White Rose Research Online URL for this paper:

<https://eprints.whiterose.ac.uk/119662/>

Version: Accepted Version

Article:

Salavagione, H. J., Sherwood, J. orcid.org/0000-0001-5431-2032, De Bruyn, M. orcid.org/0000-0002-9687-1606 et al. (4 more authors) (2017) Identification of high performance solvents for the sustainable processing of graphene. *Green Chemistry*. pp. 2550-2560. ISSN 1463-9262

<https://doi.org/10.1039/c7gc00112f>

Reuse

Items deposited in White Rose Research Online are protected by copyright, with all rights reserved unless indicated otherwise. They may be downloaded and/or printed for private study, or other acts as permitted by national copyright laws. The publisher or other rights holders may allow further reproduction and re-use of the full text version. This is indicated by the licence information on the White Rose Research Online record for the item.

Takedown

If you consider content in White Rose Research Online to be in breach of UK law, please notify us by emailing eprints@whiterose.ac.uk including the URL of the record and the reason for the withdrawal request.



Identification of High Performance Solvents for the Sustainable Processing of Graphene

Journal:	<i>Green Chemistry</i>
Manuscript ID	GC-ART-01-2017-000112
Article Type:	Paper
Date Submitted by the Author:	10-Jan-2017
Complete List of Authors:	<p>Salavagione, Horacio; Instituto de Ciencia y Tecnología de Polímeros (ICTP), CSIC, Dept. Polymer Physics, Elastomers & Energy</p> <p>Sherwood, James; University of York, Green Chemistry Centre of Excellence</p> <p>De bruyn, Mario; University of York,, Department of Chemistry,</p> <p>Budarin, Vitaliy; University of York,, Department of Chemistry,</p> <p>Ellis, Gary; ICTP, Polymer Physics</p> <p>Clark, James; University of York, Chemistry; The University of York</p> <p>Shuttleworth, Peter; Instituto de Ciencia y Tecnología de Polímeros, CSIC, Departamento de Física de Polímeros, Elastómeros y Aplicaciones Energéticas</p>

Article type: Full paper

**Green
Chemistry**
Cutting-edge research for a greener sustainable future



Website www.rsc.org/greenchem

Impact factor* 8.506

Journal expectations To be suitable for publication in *Green Chemistry* articles must report innovative research on the development of alternative sustainable technologies demonstrating a significant advance in green and sustainable chemistry.

Article type: Full paper Original scientific work that has not been published previously. Full papers do not have a page limit and should be appropriate in length for scientific content.

Journal scope Visit the [Green Chemistry website](#) for additional details of the journal scope and expectations.

Green Chemistry provides a unique forum for the publication of innovative research on the development of alternative sustainable technologies. The scope of *Green Chemistry* is based on, but not limited to, the definition proposed by Anastas and Warner (Green Chemistry: Theory and Practice, P T Anastas and J C Warner, Oxford University Press, Oxford, 1998). Green chemistry is the utilisation of a set of principles that reduces or eliminates the use or generation of hazardous substances in the design, manufacture and application of chemical products.

Green Chemistry is at the frontiers of this interdisciplinary science and publishes research that attempts to reduce the environmental impact of the chemical enterprise by developing a technology base that is inherently non-toxic to living things and the environment. Submissions on all aspects of research relating to the endeavour are welcome.

The journal publishes original and significant cutting-edge research that is likely to be of wide general appeal. Coverage includes the following, but is not limited to:

- the application of innovative technology to establish industrial procedures
- the development of environmentally improved routes, synthetic methods and processes to important products
- the design of new, greener and safer chemicals and materials
- the use of sustainable resources
- the use of biotechnology alternatives to chemistry-based solutions
- methodologies and tools for measuring environmental impact and application to real world examples
- chemical aspects of renewable energy

All items must be written so as to be widely accessible (conceptually) to chemists and technologists as well as, for example, final year undergraduates.

Reviewer responsibilities Visit the [Reviewer responsibilities website](#) for additional details of the reviewing policy and procedure for Royal Society of Chemistry journals.

When preparing your report, please:

- Focus on the originality, importance, impact and reliability of the science. English language and grammatical errors do not need to be discussed in detail, except where it impedes scientific understanding.
- Use the [journal scope and expectations](#) to assess the manuscript's suitability for publication in *Green Chemistry*.
- State clearly whether you think the article should be accepted or rejected and include details of how the science presented in the article corresponds to publication criteria.
- Inform the Editor if there is a conflict of interest, a significant part of the work you cannot review with confidence or if parts of the work have previously been published.

Thank you for evaluating this manuscript, your advice as a reviewer for *Green Chemistry* is greatly appreciated.

Dr Sam Keltie Executive Editor
Royal Society of Chemistry, UK

Professor Walter Leitner Editorial Board Chair
RWTH Aachen University, Germany



Dr. Peter S. Shuttleworth

Instituto de Ciencia y Tecnología
de Polímeros, CSIC
c/ Juan de la Cierva, 3
28006 MADRID

Tel: (+34) 912587432
Fax +34 915644853
peter@ictp.csic.es

Green Chemistry

10th January 2017

Dear Editor,

I am writing to you regarding the submission of the manuscript “Identification of High Performance Solvents for the Sustainable Processing of Graphene” for consideration in *Green Chemistry*.

The article describes the extensive screening of more than 10,000 solvents to find a new sustainable alternative for the exfoliation of graphene. Liquid exfoliation is seen as the preferred scalable method in which to prepare graphene, and as such, any modification to this method to increase either graphene concentration or sustainability would be seen as highly significant. As a result of our effort we have found that the use of CyreneTM, a bio-based solvent derived from cellulose, could achieve graphene dispersions an order of magnitude higher than that found for NMP (the traditional graphene exfoliation solvent) under identical processing conditions. We specifically focus on a fast processing time of 15 minutes, as after consultation with various industries it is of commercial interest that processing should be as quick and simple as possible. With higher processing times we have also shown that even higher graphene concentrations of graphene can be obtained, with important minimal defects to the graphene flakes.

Further investigation into why the solvent CyreneTM yielded such high graphene dispersions identified optimal surface tension, near ideal Hansen polarity, and a higher than typical viscosity as responsible. Using these findings led to a number of other solvents being identified as sustainable, high performance solvents, further verifying the novel methodology we have developed and its results.

We believe this work is of real interest to the readers of *Green Chemistry* for a number of reasons. There are an increasing number of papers published on the topic of graphite exfoliation to graphene and its use. However, very few report on needed ‘green’ processing solvents in this area, and none have screened such an extensive amount. Therefore, we believe this publication is timely and will help direct researches and industry in the multidisciplinary field of graphene use to a more sustainable solvent choice.

We appreciate your time in considering this manuscript and please do not hesitate to contact me if you require any further information, and I look forward to hearing from you in due course.

The article (Microsoft word 2010) includes 5 figures (file format: tif), and also references to two supplementary files (Microsoft word and excel).

Yours sincerely,

Dr. Peter S. Shuttleworth, Ph.D

(On behalf of the other corresponding author, **Prof. James H. Clark** and authors)



Journal Name

ARTICLE

Received 00th January
20xx,

Identification of High Performance Solvents for the Sustainable Processing of Graphene

H.J. Salavagione,^a J. Sherwood,^b M. De bruyn,^b V.L. Budarin,^b G.J. Ellis,^a J.H. Clark*^b and P.S. Shuttleworth*^a

Accepted 00th January 20xx

DOI: 10.1039/x0xx00000x

www.rsc.org/

Nanomaterials have many advanced applications, from bio-medicine to flexible electronics to energy storage, and the broad interest in graphene-based materials and devices means that high annual tonnages will be required to meet this demand. However, manufacturing at the required scale remains unfeasible until economic and environmental obstacles are resolved. Liquid exfoliation of graphite is the preferred scalable method to prepare large quantities of good quality graphene, but only low concentrations are achieved and the solvents habitually employed are toxic. Furthermore, good dispersions of nanomaterials in organic solvents are crucial for the synthesis of many types of nanocomposites. To address the performance and safety issues of solvent use, a bespoke approach to solvent selection was developed and the renewable solvent Cyrene was identified as having excellent properties. Graphene dispersions in Cyrene were found to be an order of magnitude more concentrated than those achieved in N-methylpyrrolidinone (NMP). Key attributes to this success are optimum solvent polarity, and importantly a high viscosity. We report the role of viscosity as crucial for the creation of larger and less defective graphene flakes. These findings can equally be applied to the dispersion of other layered bi-dimensional materials, where alternative solvent options could be used as drop-in replacements for established processes without disruption or the need to use specialized equipment. Thus, the discovery of a benign yet high performance graphene processing solvent enhances the efficiency, sustainability and commercial potential of this ever-growing field, particularly in the area of bulk material processing for large volume applications.

Introduction

The manufacture of nanocomposite materials is commonly achieved through wet impregnation techniques, where the nanomaterial is dispersed in a solvent that is subsequently removed. Graphene has generated substantial interest in recent years due to its unique combination of excellent mechanical, electrical, thermal and optical properties,¹ making it an interesting material for a great number of varied applications, including flexible electronics,^{2,3,4} energy storage,^{5,6,7,8} corrosion inhibition,⁹ etc. The different methods of graphene fabrication each have advantages and disadvantages. So-called 'bottom-up' approaches such as chemical vapor deposition (CVD) are useful for assembling precision, high value materials, electronics being one example.¹⁰ Conversely, the 'top-down' approach has broader utility, and is relevant to the bulk processing of two-

dimensional materials for nanocomposites for instance. As an example of a 'top-down' approach, liquid exfoliation methods (from graphite) are cheap, versatile, simple to execute, and therefore scalable.^{11,12} Advantageously, in many cases the resulting dispersion can be directly applied to the synthesis of composite materials. Unfortunately yields can be low, both in terms of the quantity of single layer graphene sheets obtained and the amount of remaining unexfoliated material.¹³ The issue of low yields has been addressed with long processing times under sonication, the use of electrochemical processes, addition of surfactants, etc. to assist the exfoliation process. However, these strategies can result in significant deterioration in the structural quality of the material, or an increase in the number of processing steps, leading to a less useful product.¹⁴

Moreover, a fundamental problem with liquid phase exfoliation and dispersion (relevant to sonication and shear methods) is that the preferred solvents present quite severe health risks, as typified by the reproductive toxicants NMP and DMF.^{15,16,17} Both have been placed on the candidate list of 'Substances of Very High Concern' (SVHC), the prerequisite step to any substance becoming restricted and subject to authorization under European REACH regulation [Regulation (EC) N^o. 1907/2006] before use or import into Europe is permitted.¹⁸ In the USA similar concerns over NMP,¹⁹ and DMF,²⁰ have been raised. Thus, it follows that these solvents

^a Departamento de Física de Polímeros, Elastómeros y Aplicaciones Energéticas, Instituto de Ciencia y Tecnología de Polímeros, CSIC, c/ Juan de la Cierva, 3, 28006, Madrid (Spain).

^b Email: peter@york.ac.uk

^c Green Chemistry Centre of Excellence, University of York, Heslington, York, Yorkshire, YO10 5DD (UK).

^d Email: james.clark@york.ac.uk

† Electronic Supplementary Information (ESI) available: [details of any supplementary information available should be included here]. See DOI: 10.1039/x0xx00000x

are an unsustainable option for graphene processing. Unfortunately viable substitutes for these dipolar aprotic solvents are scarce. One alternative solvent is 1,2-dichlorobenzene (oDCB),²¹ as it is not currently subject to REACH restrictions. However, it appears on the international ChemSec 'SIN (Substitute It Now) list',²² and the US EPA 'Extremely Hazardous Substances List' due to its high aquatic toxicity.²³

When considering other solvent systems, low boiling volatile organic compounds (VOCs) are appealing from a processing perspective, but these remain unpopular because the amount of graphene obtained in dispersion is typically halved,²⁴ or they require the transfer of graphene from a suspension in NMP anyway.²⁵ Instead of organic solvents, liquid exfoliation of graphite is also possible in aqueous media employing surfactants.²⁶ However, only certain planar or disk-like surfactants are pertinent, and if used for the manufacture of composite materials the residual surfactant on the graphene may affect their resulting properties. Moreover, these surfactants are typically insulating which leads to costly cleaning steps after film formation or device manufacture. Graphene has also been prepared via electrochemical techniques,²⁷ including the use of aqueous electrolytes.^{28,29} Compared to ultrasound assisted exfoliation of graphite, these methods require specialized equipment and additional steps to isolate the graphene laminates, and typically lead to high defect ratios. The anodic polarization of graphite electrodes, causing delamination and the formation of solid deposits, is potentially scalable but the resulting material is oxidized and therefore requires further processing steps to achieve a better quality material.^{29,30} Cathodic polarization gives higher quality graphite intercalation compounds, but ultimately exfoliation with additional ultrasound treatments in organic solvents like NMP and DMF is still required to produce a useable graphene material.^{31,32}

It is clear that any dependence on conventional solvents will hinder the long term development and sustainability of the graphene nanocomposite industry, but alternatives to liquid exfoliation have not yet been developed to the point where they are relevant for the mass production of graphene or other two dimensional materials. New solvents are urgently needed that overcome the toxicity issues of the high performance solvents used today, but this must not be achieved by compromising on performance. In response to this challenge, we now report the discovery of a sustainable solvent for the liquid phase exfoliation of graphite, and provide a rationalization for the high concentration of graphene observed. The identification of benign, high performance solvent candidates was achieved computationally by matching solvents to a set of ideal characteristics required for successful graphene dispersion, which include polarity, surface tension, viscosity, toxicity and "greenness". Considering the current growth in the technological areas that are set to benefit from the use of nanomaterials, demand for large quantities of benign processing solvents compliant with the relevant regulations must be met to secure the future of this burgeoning industry. Our technique of solvent selection is

equally applicable to the dispersion of other two dimensional materials for bulk processing applications, signifying that solvents can be found that are beneficial at all stages of research and development, and through to commercialization, for a large number of advanced products.

Experimental

Graphene dispersion procedure

Solvent was added (3 mL) to a vial containing ~ 4.5 mg of graphite (Aldrich, <45 micron, 99.99%, B.N. 496596-113.4G). The mixture was treated with an ultrasonic probe during 15 minutes and the dispersions were centrifuged at 7000 rpm for 10 minutes. The supernatant was pipetted out and used for the subsequent studies.

UV calibration

A centrifuged sample of graphene in Cyrene (1 mL) was passed through a fluoropore™ membrane (0.2 μm pore size) and the solid residue carefully weighed, accounting for any residual solvent to determine the actual dispersion of graphene. The same solution was diluted several times in order to prepare samples with different graphene amounts to collect the absorption spectra.

High resolution transmission electron microscopy (HRTEM)

Dispersions of both Cyrene and NMP were analyzed at the Centro Nacional de Microscopía Electrónica, Madrid, Spain with the aid of a technician. HRTEM micrographs were taken at random locations across the grids, to ensure a non-biased assessment. For measurement of graphene flake lateral dimensions, a JEOL JEM-2100 instrument (JEOL Ltd., Akishima, Tokyo, Japan), using a LaB6 filament, a lattice resolution of 0.25 nm and an acceleration voltage of 200 kV was used. Analysis of the graphene flake layers and molecular integrity were carried out on a JEOL JEM-3000F instrument (JEOL Ltd., Akishima, Tokyo, Japan), using a LaB6 filament, a lattice resolution of 0.17 nm and an acceleration voltage of 300 kV. Directly after sonication and centrifugation the dispersion was added to an equal volume of acetone to dilute it as it was found that it was too concentrated to achieve a good TEM image, and secondly to aid evaporation of the solvent. Samples were prepared by drop-casting a few milliliters of dispersion onto holey carbon films (copper grids) and dried at 120 °C under vacuum for 12 hours.

Raman spectroscopy

Measurements were undertaken in the Raman Microspectroscopy Laboratory of the Characterisation Service in the Institute of Polymer Science & Technology, CSIC using a Renishaw InVia-Reflex Raman system (Renishaw plc, Wotton-under-Edge, UK), which employed a grating spectrometer with a Peltier-cooled CCD detector coupled to a confocal microscope. The Raman scattering was excited with an argon ion laser ($\lambda = 514.5$ nm), focusing on the sample with a 100x microscope objective (NA=0.85) with a laser power of approximately 2 mW at the sample. Spectra were recorded in the range between 1000 and 3200 cm^{-1} . All spectral data was processed with Renishaw WiRE 3.3 software.

Solvent polarity

Hansen solubility parameter calculations were conducted with the HSPiP software package (4th Edition 4.1.04, developed by Abbott, Hansen and Yamamoto).

Results and Discussion

Bio-based Cyrene as a high performance solvent for graphene

There has been much discussion over the exact role of the solvent in the processing of carbon nanostructures, which is still open to debate.^{33,34,35} Regarding graphene dispersions, the consensus is that the solvent surface energy is of crucial importance,^{17,36} and observations that concentration correlates to solvent polarity should also be considered as highly significant.^{37,38} If this is true then it should be possible to select a number of non-toxic, alternative solvents based on a screening of potential candidates. However, it may also be the case that other solvent properties, previously overlooked, could also be jointly responsible for the efficiency of the process. By implementing a methodical solvent selection procedure, substitute solvents can be proposed and tested. Carrying out this process improves our understanding of liquid exfoliation methods, and can lead to other relevant properties being identified from the solvent dataset (should they exist).

Cyrene (CAS: 53716-82-8) is derived in 2 simple steps from cellulose *via* levoglucosenone,³⁹ and was recently reported as a replacement solvent for organic transformations where NMP is currently the favored solvent.⁴⁰ This multifunctional, bio-based solvent is composed of 2 fused rings (see Figure 1a and the Supporting Information, Scheme S1) and importantly it does not contain the amide functionality associated with the reproductive toxicity of many of the common dipolar aprotic solvents (*e.g.* NMP and DMF). Equally, Cyrene does not contain any chlorine which can present end-of-life pollution issues or create corrosive by-products if incinerated (*e.g.* *o*DCB). We can report that Cyrene has very low acute toxicity (LD_{50}) and aquatic toxicity (EC_{50}) values of $>2000 \text{ mg kg}^{-1}$ and $>100 \text{ mg L}^{-1}$ respectively. These are well above the hazard thresholds defined by the Globally Harmonized System of Classification and Labelling of chemicals (GHS),⁴¹ also adopted as European Regulation (EC) 1272/2008 (classification, labelling and packaging (CLP) of substances).⁴² Additionally Cyrene is biodegradable, not mutagenic, and with a flash point of $108 \text{ }^\circ\text{C}$ it is safer to handle than many oxygenated solvents. It is stable to oxidation and (at end-of-life) upon incineration or biodegradation yields only carbon dioxide and water. This is an advantage over equivalent petrochemical dipolar aprotic solvents such as NMP which liberate NO_x upon decomposition. Dispersions of graphene were generated by applying 15 minutes of ultrasound treatment to aid graphite exfoliation separately in both Cyrene and NMP, followed by 10 minutes of centrifugation at 7000 rpm. The short ultrasound duration was chosen bearing in mind industrial productivity of the process, with longer times seen as a key limiting factor when scaling. It is also known to be sufficient to aid graphene-solvent dispersion, but also brief enough to limit solvent degradation

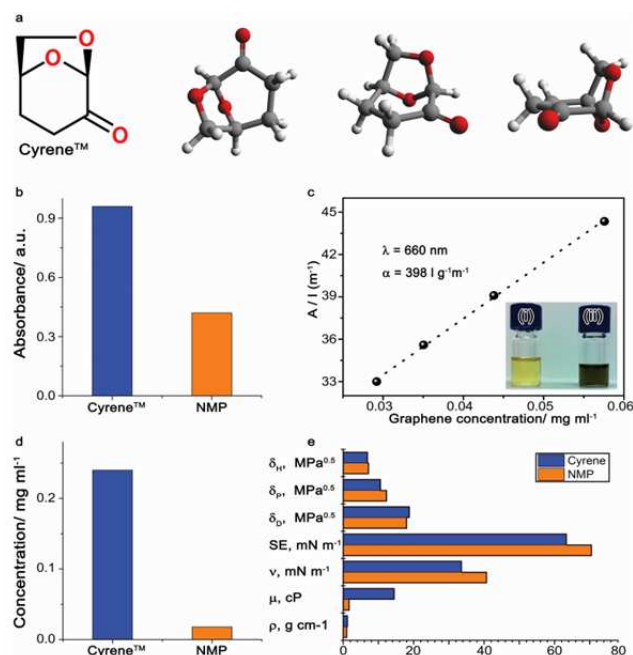


Figure 1. Comparison of NMP and Cyrene. (a) Molecular structure of Cyrene™ and 3D representations. (b) The magnitude of UV-visible spectrum absorbances of graphene dispersions in the solvents Cyrene and NMP at 660 nm. (c) Optical absorbance ($\lambda_{ex} = 660 \text{ nm}$) divided by cell length (A/l), as a function of graphene concentration in Cyrene. The concentration range chosen reflects results in NMP. The inset picture (bottom right) shows samples of (i) pure Cyrene and (ii) Cyrene dispersed graphene. (d) The concentration of graphene achieved in Cyrene and NMP. (e) The physical properties of Cyrene compared to NMP.

and subsequent formation of oligomers or polymers that can then adhere or radically graft to the nanoparticle surface, further stabilizing them in solution.^{43,44} The concentration of dispersed graphene in the supernatant was then measured using UV spectroscopy in accordance with established methods as defined by Hernandez *et al.*,¹⁷ with full details of materials and methods presented in the Supporting Information. Using the standard UV absorbance at 660 nm ,¹⁷ where the spectra of the NMP and Cyrene graphene dispersions both have a gradient of approximately zero, the observed magnitudes of absorbance are 0.42 and 0.96 respectively (see Figure 1b). Figure 1c displays the linear correlation fit according to the Lambert-Beer law required to calculate the molar absorptivity coefficient. A value of $398 \text{ L g}^{-1} \text{ m}^{-1}$ was obtained, which is similar to reports for other carbon nanostructures, but somewhat lower than previously reported for graphene dispersed in different solvents as a result of similar treatments.^{17,45,46} For dispersed carbon nanostructures the absolute value depends on the different number of layers and the surface properties of the graphene.^{47,48} An insight into the number of layers and the size of the graphene flakes after dispersion in Cyrene is provided later. Using the experimentally derived molar absorptivity coefficient for Cyrene, the concentration of dispersed graphene was found to be 0.24 mg mL^{-1} . This is an order of magnitude greater than observed for the commonly used solvent NMP (0.018 mg mL^{-1}) using its standard molar absorptivity coefficient of $\alpha = 2460 \text{ L g}^{-1} \text{ m}^{-1}$ under exactly the same experimental conditions (see Figure 1d).¹⁷ This substantial increase in the achievable concentration of graphene, without the use of surfactants and with a short processing time, has

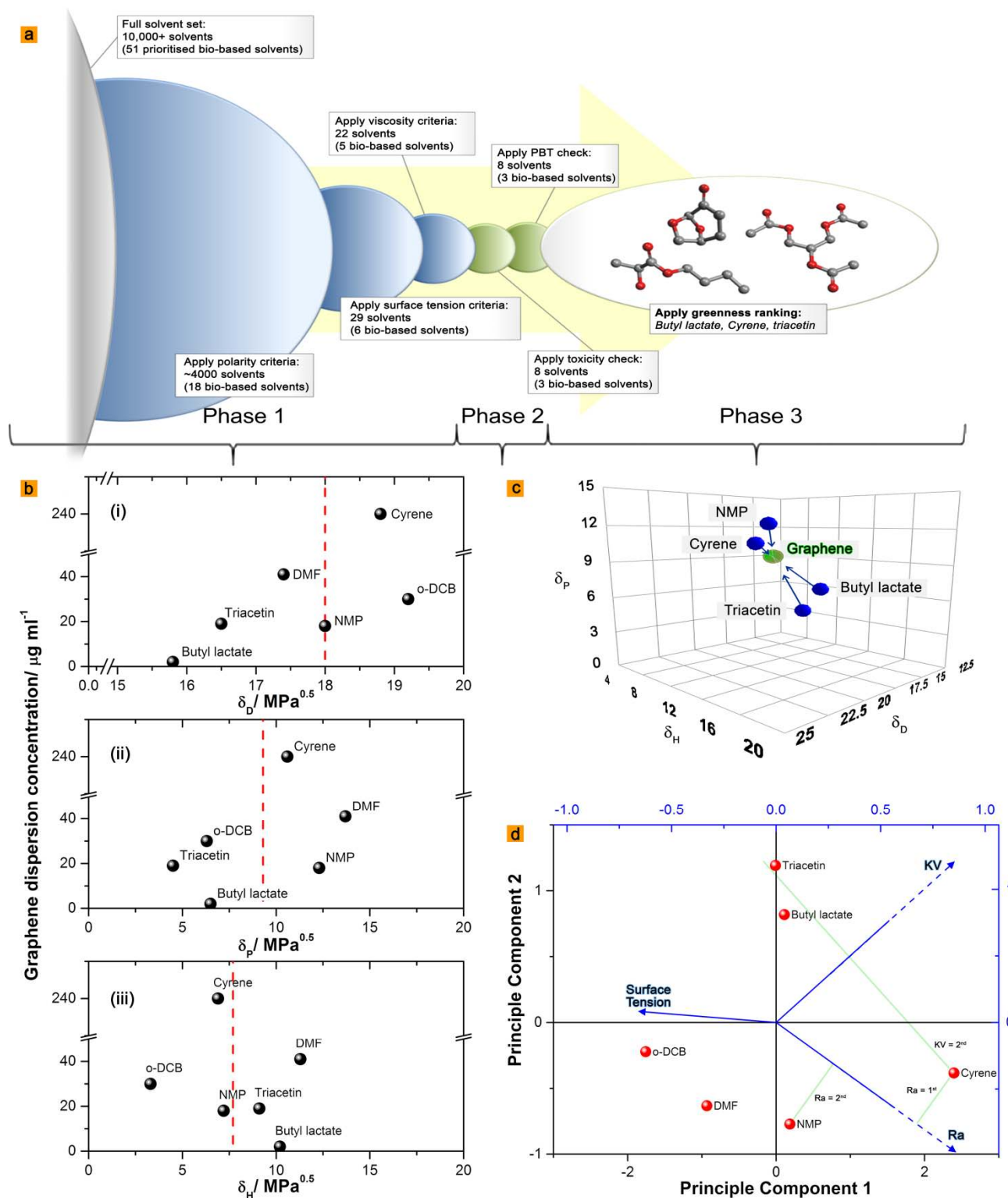


Figure 2. The application of solvent selection criteria for optimizing graphene dispersions. (a) Pictorial representation of the solvent selection steps applied for the computational screening of suitable solvents. (b) Graphene dispersion as a function of (i) dispersive, δ_D (ii) polar, δ_P and (iii), hydrogen-bonding, δ_H Hansen solubility parameters, with the dashed red line being indicative of ideal graphene properties. (c) Hansen solubility map showing the similarity of the final bio-based solvent candidates (and NMP) to graphene in terms of their polarity. (d) Principle Component Analysis (PCA) biplot for candidate solvents (including NMP, oDCB and DMF for reference) with vectors (lines with arrow heads) indicating surface tension; kinematic viscosity (KV), where high viscosity and a reduced settling velocity according to Stokes' law are beneficial; and Hansen radius (Ra). The values of the selected solvent parameters were normalized for the PCA, with the value for Ra presented as lower values giving higher scores. The projection lines perpendicular to the vector lines show that Cyrene has the lowest Ra and second highest kinematic viscosity.

important implications for the efficiency of future large scale processing, suggesting that higher throughput, reduced waste and lower energy consumption is possible, which in turn could

have an impact on the market price of graphene products. Also, this could extend the number of commercially viable graphene applications to include high volume products such as

composites, energy storage, biomedical devices, and coatings to name but a few.⁵⁰ The preparation conditions were optimized (as presented subsequently) to achieve graphene concentrations in the region of $\approx 1.0 \text{ mg mL}^{-1}$, still using one simple processing step (see Supporting Information, Figure S10).

Rationalization of solvent selection for graphene processing

After establishing a comparison between the properties of NMP and Cyrene, it was surprising to observe how much more concentrated the graphene dispersions were in Cyrene. It would have been expected that the ideal solvent for graphene processing would have similar physical properties to NMP for example, but with an improved environmental, health and safety profile. This is true of Cyrene, but does not explain the vast difference in its performance, compared to NMP. Some relevant characteristics of Cyrene compared to those of NMP are provided in Figure 1e. The only notable distinction between the physical properties of Cyrene and the conventional solvents used for producing graphene is in their viscosities.

Cyrene is indeed more viscous than most solvents in regular use (Figure 1e), and this may be responsible in part for the high concentration of dispersed graphene achieved. This hypothesis led to us to develop a more comprehensive solvent selection procedure, firstly to generate more sustainable solvent candidates (for graphene processing in this instance), and secondly to construct a rationale with which to better describe and understand solvent performance. It was our intention to create a solvent selection methodology based on generalized principles so that it may find use in other applications, such as other bidimensional/layered crystal materials where otherwise an extensive regime of costly and time consuming screening experiments would be needed.

To assess the role of surface tension, polarity, and viscosity in detail, a database of more than 10,000 solvents (containing 51 bio-based solvents) was screened against the extended physical property criteria (phase 1), followed by toxicity, then environmental persistency, bioaccumulation, and aquatic toxicity (phase 2) through a series of stage gates (see Figure 2a for a summary of the screening procedure), as fully explained in the Supporting Information. Algorithms for solvent selection have been used previously to optimize extractions, reaction chemistry,⁵¹ and for the selection of green alternative solvent pairs for polymer synthesis,⁵² but to date this approach has not been extended to the more complex problem of graphite exfoliation and dispersion. By applying our algorithm the large dataset was refined to just 8 solvents that both satisfied all of the physical property requirements and were compliant with REACH.

Thus, after screening (phase 1 and phase 2), the solvents identified as potentially high performance solvents for greener graphene processing were: Cyrene, *o*DCB, benzonitrile, butyl lactate, cyclohexanone, cyclopentanone, pyridine, and triacetin. In principle, NMP and DMF did fulfill the property requirements (phase 1) but are unsuitable based on their reprotoxicity (phase 2). To the best of the authors' knowledge,

this is the outcome of the most comprehensive attempt yet to rationalize solvent selection for graphene dispersions, and crucially without the restriction of being limited to observations based on a small experimental set of solvents.

Reviewing the eight-solvent shortlist with environmental health and safety principles in mind (phase 3), butyl lactate and triacetin emerged, along with Cyrene, as the most promising green solvents. As well as being the only solvents to satisfy the requirements of the complete solvent selection procedure, all three are renewable, and none are considered flammable, acutely toxic, or harmful to the aquatic environment according to European CLP regulation.⁴² It is worth noting that cyclohexanone and cyclopentanone have been suggested as green graphene processing solvents previously.³⁷ However both have low flash points and for this reason failed phase 3 of the solvent selection procedure. The solvents 1,2-dichlorobenzene, benzonitrile, and pyridine (like cyclohexanone and cyclopentanone) are also non-renewable but, more importantly, they are all acutely toxic.

As a preliminary verification of the suitability of our solvent candidates, contact angles measurements on graphene were obtained (Supporting Information, Figure S3). Butyl lactate and especially triacetin displayed non-ideal wetting, and to a lesser extent this was also true for Cyrene. Nevertheless, the viscous triacetin provided a suitable medium for graphene dispersions that was found to be approximately equivalent to NMP in terms of the concentration achieved (0.019 mg mL^{-1}), again highlighting limitations in the use of contact angles alone to identify suitable solvents for graphite exfoliation. Figure 2b shows the values of the Hansen solubility parameters for the three preferred solvents (including NMP, *o*DCB and DMF as further reference solvents), versus the concentration of dispersed graphene that was obtained. The accepted Hansen solubility parameters for graphene, $\delta_D = 18.0 \text{ MPa}^{0.5}$, $\delta_P = 9.3 \text{ MPa}^{0.5}$, $\delta_H = 7.7 \text{ MPa}^{0.5}$, are indicated on these charts, with ideal solvents having a similar polarity.³⁷ The dispersion solubility parameter (δ_D) of NMP is almost identical to that of graphene, with Cyrene and *o*DCB being slightly higher. Effective solvents for graphite exfoliation have non-zero polarity (δ_P) and hydrogen bonding (δ_H) values despite the non-polar nature of graphene, and all three Hansen solubility parameters are essential when describing the affinity between solvent and solute. Cyrene presents similar δ_H compatibility and the closest δ_P match to graphene. A 3D representation illustrates how the solvents compare to graphene from their distance in Hansen space (see Figure 2c). A key finding is that of all the solvents found to meet the performance criteria (phase one), Cyrene has the smallest Hansen radius (the distance from graphene in the Hansen space, $2.2 \text{ MPa}^{0.5}$), hence suggesting the greatest affinity to graphene.

Further analysis of the identified solvent parameters (i.e. surface tension, viscosity and Hansen radius), was undertaken using Principle Component Analysis, PCA (Figure 2d). This technique suggested that the surface tension of the solvent appears to have the least specific role of the three parameters, but is still vital for graphene processing. If the surface tension is sufficient to promote a general affinity towards graphene,

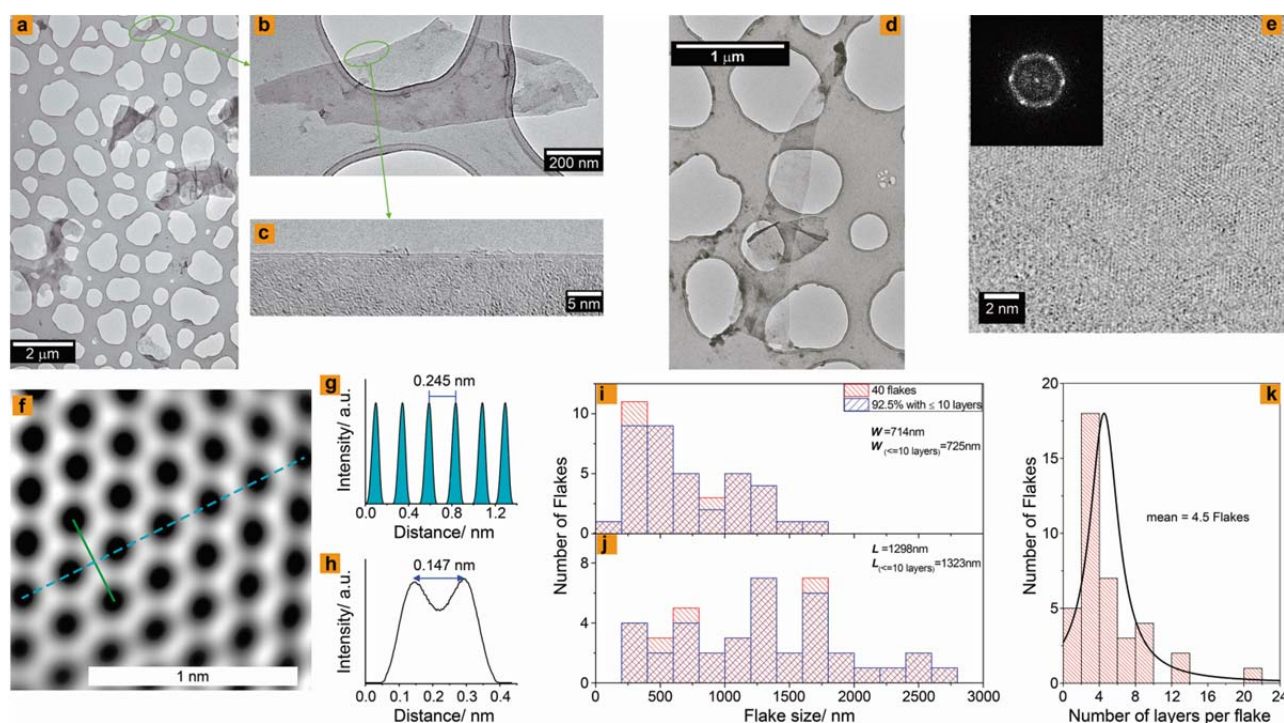


Figure 3. TEM analysis of Cyrene dispersed graphene. (a) TEM of a holey carbon grid coated with a number of graphene flakes. (b) A TEM image of a single graphene flake. (c) Magnification of the border area of the flake displayed in (b) showing it to be mono- or bi-layer. (d) An example of a larger single graphene flake, possibly with some folding and a smaller flake underneath. (e) HRTEM of monolayer graphene as confirmed by the FFT diffraction pattern of the image showing a set of six inner spots and much less intense outer spots (inset) with a well-defined grain structure. (f) A filtered image of the region shown in (e) allowing the well-defined graphene hexagon structure to be observed. (g) Intensity analysis along the dashed line presented in (f). (h) Intensity profile along the green line in (f) of a C-C bond length. (i, j and k) Histograms showing the size distribution of the graphene flakes width, length and layer thickness respectively.

only then do solvent polarity and viscosity have the opportunity to enhance the process efficiency. For example, Cyrene has a superior polarity to triacetin whilst being similarly viscous, therefore the concentration of graphene observed in triacetin dispersions is the lower of the two, but nevertheless still comparable to NMP. Butyl lactate is less viscous than triacetin, again more similar to NMP, but in terms of its polarity not as suitable as NMP. For these reasons the concentration of graphene generated in butyl lactate is low but measurable (0.002 mg mL^{-1}).

Analysis of exfoliation and graphene quality

As described above, the effectiveness of Cyrene for preparing stable graphene dispersions in high yield has been corroborated and explained based on the physical properties of the studied solvents. However, it is also necessary to evaluate the quality of the dispersed graphene. The lateral dimensions of the graphene flakes were thoroughly evaluated using high resolution transmission electron microscopy (HRTEM). Representative results are presented in Figure 3 extracted from images of Cyrene dispersions deposited on holey carbon grids, collected at forty different points (experimental details along with the results of NMP can be found in the Supporting Information, Figure S5). As expected some heterogeneity is perceived in both the lateral dimensions of the flakes and their thickness. Figure 3a shows a low magnification TEM image demonstrating a typical distribution of flakes seen with lateral dimensions in this case between 450 nm and $3 \mu\text{m}$. From Figure 3a, a close-up of a graphene flake with lateral dimensions in the range of $1.25 \times 0.45 \mu\text{m}^2$ is

shown (Figure 3b), with increased magnification at its border (Figure 3c) demonstrating it to be a monolayer with well-defined edges. A larger example of a monolayer ($2.9 \times 0.3 \mu\text{m}^2$) flake can be seen in Figure 3d. Figure 3e shows a HRTEM image of another graphene monolayer with its respective fast Fourier transform (FFT) diffraction pattern (inset), displaying the characteristic more intense inner $\{0-110; -1010\}$ spots and fainter outer $\{1-210; -2110\}$ ones, confirming the existence of a single layer.^{17,53} Applying a filter to this image (Figure 3f) permits the hexagonal defect-free structure of graphene from its intensity analysis (Figure 3g) to be assessed with a measured hexagon width of 0.25 nm (dashed blue line) found, very close to other reported values.^{54,55} Likewise, analysis of the intensity profile along the green line in Figure 3f allows the C-C bond length of 1.47 Å to be estimated (Figure 3h), close to the expected value of 1.42 Å.

In addition, folded flakes as well as flakes thicker than monolayer graphene (bilayer, three-layer, few-layers and multilayers) were also observed for both Cyrene and NMP generated graphene. Statistical analysis demonstrates that the average length and width of the flakes (≤ 10 layers) produced using Cyrene are larger than those made using NMP under identical conditions (see Figure 3i, j and Supporting Information, Figure S7). The mean dimensions of the ≤ 10 layer flakes dispersed in Cyrene were measured as $0.725 \pm 0.406 \mu\text{m}$ in width and $1.323 \pm 0.647 \mu\text{m}$ in length compared to $0.520 \pm 0.450 \mu\text{m}$ and $0.831 \pm 0.595 \mu\text{m}$ respectively measured for NMP.

To ascertain the thickness of the flakes, further statistical analysis across the entirety of the TEM images was performed,

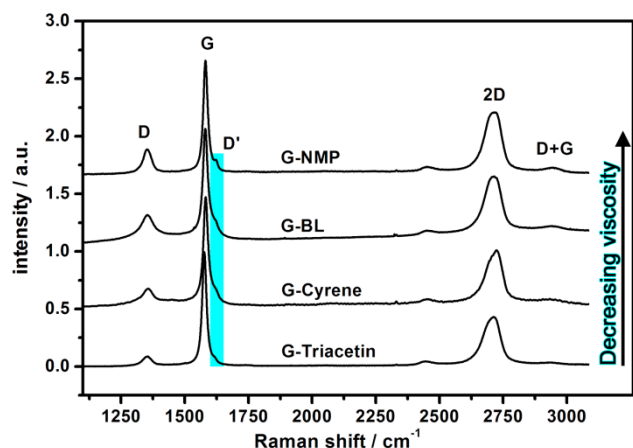


Figure 4. Figure Raman spectra of drop-casted graphene films ($\lambda_{\text{laser}} = 2.41$ eV). Films were prepared using NMP (G-NMP), Butyl lactate (G-BL), Cyrene (G-Cyrene) and triacetin (G-Triacetin) and are presented in order of most viscous (triacetin, bottom) to least viscous solvent (NMP, top). The G band (a primary E_{2g} in-plane vibration mode), the disorder-induced D and D'-bands, the second-order 2D (or G') band of the graphene spectra are labelled for clarity. For more information on graphene Raman spectroscopy please refer to Malard *et al.*⁵⁶

counting the number of layers at the edge of sheets by HRTEM. The results indicated that 92.5 % of the flakes produced using Cyrene has 10 or fewer layers. Furthermore, 75% had no more than 5 layers and 7.5% are monolayer graphene, with the mean flake layer count being 4.5 per flake (Figure 3k). On a mass basis, the monolayer flakes account for 1.2% of the sample, while few-layer (≤ 5) graphene flakes make up approximately 10% of the sample mass. Compared to samples produced in NMP, those produced with Cyrene are much thinner on average, with only 42.5% of the flakes produced using NMP composed of ≤ 10 layers, suggesting that the NMP dispersion was still largely graphitic. In the case of NMP exfoliated graphite no monolayer flakes were detected under the conditions specified. One of the most important features in 2D materials like graphene is a high aspect ratio. Using the mean lengths and thicknesses obtained from the TEM images, and the known interlayer distance between graphene layers of 0.345 nm, the average aspect ratio of graphene prepared in Cyrene was much higher than NMP and estimated to be approximately 1000 and 600, respectively.

Raman spectroscopy was also applied to further assess graphene quality and evaluate the influence of solvent viscosity. Extending the comparison to NMP provided a benchmark for evaluating the quality of the graphene dispersed in butyl lactate, Cyrene, and triacetin. The most important features in the Raman spectra, as shown in Figure 4, are the G band, a primary E_{2g} in-plane vibration mode appearing around 1582 cm⁻¹, the second order 2D band at around 2700 cm⁻¹ and the disorder-induced D and D' bands around 1350 cm⁻¹ and 1620 cm⁻¹, respectively. The first-order G-mode and D-mode appear at the same frequencies in graphene produced in either NMP or Cyrene, and the average full width at half maximum (FWHM) of the D-band is 39.8 cm⁻¹ and found to be identical for both samples. However, more revealing is the A_D/A_G ratio, which is a known probe of structural defects in the carbon network.⁵⁷ A_D/A_G ratios were calculated by collecting Raman spectra at 20 different points for each sample. This ratio decreases from 0.29 ± 0.08 for NMP

to 0.20 ± 0.06 for Cyrene, providing evidence of less defective graphene flakes when using Cyrene as the dispersing solvent, and hence, further supporting the importance of viscosity.

Analysis of the Raman I_D/I_G ratio (intensity) for NMP, butyl lactate, Cyrene and triacetin generated graphene dispersions shows that the mean in-plane crystallite size, L_a , of graphene particles decreases with lower solvent viscosity (see Supporting Information, Figure S9a). Average L_a values of 227 ± 76 nm and 136 ± 46 nm were obtained for the Cyrene and NMP dispersions, respectively, using the general equation proposed by Caçado *et al.*⁵⁸ The solvent viscosity also correlates to the distance between defects, L_D , and the density of these defects, n_D .⁵⁷ Both measurements are additional markers of the quality of the materials. The distance between defects, n_D is advantageously maintained in higher viscosity solvents, reducing from 40.6 ± 6.4 nm for graphene generated in Cyrene, to 31.6 ± 5.6 nm when NMP is employed. As a consequence, the density of defects increases with decreasing solvent viscosity (Supporting Information, Figure S9c). Values of $2.1 \times 10^{10} \pm 5.8 \times 10^9$, and $3.6 \times 10^{10} \pm 1.3 \times 10^{10}$ defects per cm² were calculated for Cyrene and NMP respectively.

In the related work of Kim and Lee,³⁵ the reported yield of exfoliated graphite nanosheets was found to be proportional to the solvent viscosity, and the average graphene flake thickness associated with the surface tension of the solvent. Unfortunately no explanation for the observed influence of viscosity was provided at that time. Our observations indicate that graphene particles are better protected from damage during ultrasound treatment in more viscous solvents, leading to larger and less defective flakes. This is consistent with the inverse relationship between the ultrasound velocity in a fluid (relevant to the initial preparation of the dispersions described here) and the viscosity of the solvent.⁵⁹ This is especially true at the beginning of the preparation procedure, when thermal agitation does not have enough time to exert an influence. We proved this experimentally by varying the duration of the ultrasound step, up to a maximum exposure time of 120 minutes. Whilst longer sonication times are known to increase the overall yield of the dispersed graphene, they can also be detrimental to both the size,¹³ and quality of the flakes.¹⁴ As expected, the amount of graphene dispersed in Cyrene increased gradually with sonication time, with a concentration of ~ 0.7 mg mL⁻¹ achieved after 2 hours (Figure 5a) with a very high $\sim 48\%$ graphite to graphene conversion; this is higher than what is typically obtained in different organic solvents requiring much more complex protocols.¹¹

Perhaps more importantly, the quality of the graphene resulting from varied sonication times was assessed by Raman spectroscopy (Figure 5b), with the A_D/A_G ratio calculated from an average of 20 spectra per sample. As seen, the A_D/A_G ratio for Cyrene generated graphene slightly increased with sonication time, passing from 0.20 ± 0.06 after 15 minutes to 0.30 ± 0.10 after 120 minutes. However, the corresponding A_D/A_G ratio for the graphene generated in NMP increased much more significantly, from 0.29 ± 0.08 to 0.75 ± 0.22 after the same intervals of 15 and 120 minutes. Triacetin dispersed graphene was also evaluated, and in this case the variation

was less than that observed for Cyrene. These results reiterate that solvent viscosity has a positive effect on stabilizing and preserving the integrity of the graphene flakes when using ultrasound processing. This study shows conclusively that a short, industrially relevant sonication time of 15 minutes allows for a high throughput of high quality graphene when using Cyrene as the dispersing solvent. In instances where even greater concentrations of graphene dispersed in solution are required, increasing the initial graphite loading and the duration of sonication to a more conventional processing time (2 hours) increases yields to near 1.0 mg ml⁻¹ (Supporting Information, Figure S10), albeit at the expense of the percentage of starting material converted, and a slight detriment to product quality but, if pursued, the application of a viscous solvent becomes even more pertinent.

The overall implication therefore is of a doubly beneficial effect, as solvent viscosity not only improves the stability of the dispersion by reducing settling velocity under centrifugation according to Stokes' law,⁴⁹ but also helps to preserve the integrity of the graphene flakes. However, solvents that are too viscous tend to inhibit the deposition of graphene.⁶⁰ Therefore a compromise must be reached, since the solvent cannot be so viscous that it becomes difficult to convert the dispersions into graphene materials. It also must not be ignored that the initial requirements of surface tension and polarity (Hansen radius) must still be met, and a high viscosity is not a sole substitute for unsuitable solvent properties in other respects.

Conclusions

Cyrene has been shown to present near-ideal physical properties for graphite exfoliation and the production of graphene dispersions. This discovery has advanced our understanding of which solvent effects influence the dispersion of graphene.⁶¹ In order to understand the major attributes that characterize a high performance solvent for the liquid exfoliation of graphite to graphene, a computational assessment of >10,000 solvents was employed. The solvent selection procedure included physical properties and environmental health and safety aspects to provide an indication of the availability of optimal solvents for the exfoliation of graphite. The results led to the experimental evaluation of three bio-based, viscous solvents: Cyrene, triacetin, and butyl lactate. Under conventional ultrasound processing these were able to generate graphene with fewer defects compared to conventionally used solvents such as NMP.

The solvent selection procedure developed has the broader potential for the identification of new solvents for nanomaterial processing in general, and is not just limited to graphene. If the role of the solvent can be identified in terms of physical properties from a small experimental dataset, or even speculated from predictive calculations, solvent selection for nanomaterial dispersion is now much easier to optimize and rationalize. Where dispersions of graphene or other nanoparticles are required, optimization of performance as

well as environmental health and safety is critically important if the process is to be commercially viable on the long term. Stable, high concentration graphene dispersions in Cyrene mean shorter sonication times are possible, and less solvent is required to deliver the same quantity of nanoparticles. The selected solvent, Cyrene could easily be used as a 'slot in' replacement for other solvents developed for alternative processing techniques other than sonication, such as shear mixing, which shows promise for industrial scale up.⁶² Thus the realization of larger scale processing of graphene with higher throughput to meet the growing electronics and energy markets comes one step closer, and with the added potential benefit of vastly improved economic and environmental credentials.

Acknowledgements

Financial support from the Spanish Ministry of Economy and Competitiveness (MINECO, grants MAT2013-47898-C2-2-R, MAT2014-54231-C4-4-P and MAT2014-59674-JIN), and the Spanish Scientific Research Council, CSIC (i-LINK+0636). HJS and PSS also acknowledge the MINECO for 'Ramón y Cajal' Senior Research Fellowships. We are grateful to Circa Group Pty Ltd for the provision of levoglucosenone and L. Moity (Green Chemistry Centre of Excellence) for providing the Cyrene surface tension and viscosity data. We also thank F. Hoffmann La Roche Ltd. for the Cyrene environmental, health and safety properties, I. Muñoz from the ICTP-CSIC characterization services for helping with Raman measurements and A. Gómez Herrero from the Centro Nacional de Microscopía Electrónica for the assistance with TEM.

Notes and references

‡ Footnotes relating to the main text should appear here. These might include comments relevant to but not central to the matter under discussion, limited experimental and spectral data, and crystallographic data.

§
§§

- 1 Salavagione, H. J.; Martínez, G.; Ellis, G. *Graphene-Based Polymer Nanocomposites. In Physics And Applications Of Graphene – Experiments; Mikhailov, S., Eds.; InTech: Vienna, 2011; pp 169-192.*
- 2 Ahn, J. -H.; Hong, B. H. *Graphene for displays that bend. Nat. Nano. 2014, 9, 737-738.*
- 3 Liu, J.; Yin, Z.; Cao, X.; Zhao, F.; Wang, L.; Huang, W.; Zhang, H. *Fabrication of flexible, all-reduced graphene oxide non-volatile memory devices. Adv. Mater. 2013, 25, 233-238.*
- 4 Liu, J.; Lin, Z.; Liu, T.; Yin, Z.; Zhou, X.; Chen, S.; Xie, L.; Boey, F.; Zhang, H.; Huang, W. *Multilayer stacked low-temperature-reduced graphene oxide films: preparation, characterization, and application in polymer memory devices. Small 2010, 6, 1536-1542.*

- 5 Liu, J. Charging graphene for energy. *Nat. Nano.* **2014**, *9*, 739-741.
- 6 Cao, X.; Yin, Z.; Zhang, H. Three-dimensional graphene materials: preparation, structures and application in supercapacitors. *Energy Environ. Sci.* **2014**, *7*, 1850-1865.
- 7 Yin, Z.; Zhu, J.; He, Q.; Cao, X.; Tan, C.; Chen, H.; Yan, Q.; Zhang, H. Graphene-based materials for solar cell applications. *Adv. Energy Mater.* **2014**, *4*, 1300574.
- 8 Zhu, J.; Yang, D.; Yin, Z.; Yan, Q.; Zhang, H. Graphene and graphene-based materials for energy storage applications. *Small* **2014**, *10*, 3480-3498.
- 9 Bohm, S. Graphene against corrosion. *Nat. Nano.* **2014**, *9*, 741-742.
- 10 Tour, J. M. Top-Down versus Bottom-Up Fabrication of Graphene-Based Electronics. *Chem. Mater.* **2014**, *26*, 163-171.
- 11 Lavin-Lopez, M. P.; Valverde, J. L.; Sanchez-Silva, L.; Romero, A. Solvent-based exfoliation via sonication of graphitic materials for graphene manufacture. *Ind. Eng. Chem. Res.* **2016**, *55*, 845-855.
- 12 Zhong, Y. L.; Tian, Z.; Simon, G. P.; Li, D. Scalable production of graphene via wet chemistry: progress and challenges. *Mater. Today* **2015**, *18*, 73-78.
- 13 Ciesielski, A.; Samori, P. Graphene via sonication assisted liquid-phase exfoliation. *Chem. Soc. Rev.* **2014**, *43*, 381-398.
- 14 Khan, U.; O'Neill, A.; Lotya, M.; De, S.; Coleman, J. N. High-concentration solvent exfoliation of graphene. *Small* **2010**, *6*, 864-871.
- 15 Barwich, S.; Khan, U.; Coleman, J. N. A technique to pretreat graphite which allows the rapid dispersion of defect-free graphene in solvents at high concentration. *J. Phys. Chem. C* **2013**, *117*, 19212-19218.
- 16 Gambhir, S.; Murray, E.; Sayyar, S.; Wallace, G. G.; Officer, D. L. Anhydrous organic dispersions of highly reduced chemically converted graphene. *Carbon* **2014**, *76*, 368-377.
- 17 Hernandez, Y.; Nicolosi, V.; Lotya, M.; Blighe, F. M.; Sun, Z.; De, S.; McGovern, I. T.; Holland, B.; Byrne, M.; Gun'ko, Y. K.; Boland, J. J.; Niraj, P.; Duesberg, G.; Krishnamurthy, S.; Goodhue, R.; Hutchison, J.; Scardaci, V.; Ferrari, A. C.; Coleman, J. N. High-yield production of graphene by liquid-phase exfoliation of graphite. *Nat. Nano.* **2008**, *3*, 563-568.
- 18 European Chemicals Agency (ECHA) candidate list of Substances of Very High Concern (SVHC). Available from: <http://echa.europa.eu/candidate-list-table> (Accessed 10-01-2017).
- 19 US EPA TSCA Work Plan Chemical Risk Assessment N-Methylpyrrolidone. Available from: <https://www.epa.gov/assessing-and-managing-chemicals-under-tsca/tsca-work-plan-chemical-risk-assessment-n-0> (Accessed 10-01-2017).
- 20 US EPA hazards summary: N,N-dimethyl formamide. Available from: <https://www.epa.gov/haps/health-effects-notebook-hazardous-air-pollutants> (Accessed 10-01-2017).
- 21 Hamilton, C. E.; Lomeda, J. R.; Sun, Z.; Tour, J. M.; Barron, A. R. High-yield organic dispersions of unfunctionalized graphene. *Nano Lett.* **2009**, *9*, 3460-3462.
- 22 ChemSec, the International Chemical Secretariat, SIN list database. Available from: <http://sinlist.chemsec.org/> (accessed 10-01-2017).
- 23 United States Environmental Protection Agency (US EPA) consolidated list of chemicals subject to the Emergency Planning and Community Right-To-Know Act (EPCRA), Comprehensive Environmental Response, Compensation and Liability Act (CERCLA) and Section 112(r) of the Clean Air Act. Available from: <https://www.bnl.gov/esh/env/compliance/docs/SaraTitleList.pdf> (accessed 10-01-2017).
- 24 O'Neill, A.; Khan, U.; Nirmalraj, P. N.; Boland, J.; Coleman, J. N. Graphene dispersion and exfoliation in low boiling point solvents. *J. Phys. Chem. C* **2011**, *115*, 5422-5428.
- 25 Zhang, X.; Coleman, A. C.; Katsonis, N.; Browne, W. R.; van Wees, B. J.; Feringa, B. L. Dispersion of graphene in ethanol using a simple solvent exchange method. *Chem. Commun.* **2010**, *46*, 7539-7541.
- 26 Guardia, L.; Fernández-Merino, M. J.; Paredes, J. I.; Solís-Fernández, P.; Villar-Rodil, S.; Martínez-Alonso, A.; Tascón, J. M. D. High-throughput production of pristine graphene in an aqueous dispersion assisted by non-ionic surfactants. *Carbon* **2011**, *49*, 1653-1662.
- 27 Salavagione, H. J. Promising alternative routes for graphene production and functionalization. *J. Mater. Chem. A* **2014**, *2*, 7138-7146.
- 28 Abdelkader, A. M.; Cooper, A. J.; Dryfe, R. A. W.; Kinloch, I. A. How to get between the sheets: a review of recent works on the electrochemical exfoliation of graphene materials from bulk graphite. *Nanoscale* **2015**, *7*, 6944-6956.
- 29 Yang, S.; Lohe, M. R.; Müllen, K.; Feng, X. New-generation graphene from electrochemical approaches: production and applications. *Adv. Mater.* **2016**, *28*, 6213-6221.
- 30 Parvez, K.; Li, R.; Puniredd, S. R.; Hernandez, Y.; Hinkel, F.; Wang, S.; Feng, X.; Müllen, K. Electrochemically exfoliated graphene as solution-processable highly conductive electrodes for organic electronics. *ACS Nano* **2013**, *7*, 3598-3606.
- 31 Morales, G. M.; Schifani, P.; Ellis, G.; Ballesteros, C.; Martínez, G.; Barbero, C.; Salavagione, H. J. High-quality few layer graphene produced by electrochemical intercalation and microwave-assisted expansion of graphite. *Carbon* **2011**, *49*, 2809-2816.
- 32 Zhong, Y. L.; Swager, T. M. Enhanced electrochemical expansion of graphite for in situ electrochemical functionalization. *J. Am. Chem. Soc.* **2012**, *134*, 17896-17899.
- 33 Cheng, Q.; Debnath, S.; Gregan, E.; Byrne, H. J. Ultrasound-assisted SWNTs dispersion: effects of sonication parameters and solvent properties. *J. Phys. Chem. C* **2010**, *114*, 8821-8827.
- 34 Yousefinejad, S.; Honarasa, F.; Abbasitabar, F.; Arianzhad, Z. New LSER model based on solvent empirical parameters for the prediction and description of the solubility of buckminsterfullerene in various solvents. *J. Solution Chem.* **2013**, *42*, 1620-1632.
- 35 Kim, J. H.; Lee, J. H. Preparation of graphite nanosheets by combining microwave irradiation and liquid-phase exfoliation. *J. Ceram. Process. Res.* **2014**, *15*, 341-346.

- 36 Wang, S.; Zhang, Y.; Abidi, N.; Cabrales, L. Wettability and surface free energy of graphene films. *Langmuir* **2009**, *25*, 11078-11081.
- 37 Hernandez, Y.; Lotya, M.; Rickard, D.; Bergin, S. D.; Coleman, J. N. Measurement of multicomponent solubility parameters for graphene facilitates solvent discovery. *Langmuir* **2010**, *26*, 3208-3213.
- 38 Yi, M.; Shen, Z. G.; Zhang, X. J.; Ma, S. L. Achieving concentrated graphene dispersions in water/acetone mixtures by the strategy of tailoring Hansen solubility parameters. *J. Phys. D: Appl. Phys.* **2013**, *46*, 025301.
- 39 De Bruyn, M.; Fan, J.; Budarin, V. L.; Macquarrie, D. J.; Gomez, L.D.; Simister, R.; Farmer, T. J.; Raverty, W. D.; McQueen-Mason, S. J.; Clark, J. H. *Energy Environ. Sci.* **2016**, *9*, 2571-2574.
- 40 Sherwood, J.; De bruyn, M.; Constantinou, A.; Moity, L.; McElroy, C. R.; Farmer, T. J.; Duncan, T.; Raverty, W.; Hunt, A. J.; Clark, J. H. Dihydrolevoglucosenone (cyrene) as a bio-based alternative for dipolar aprotic solvents. *Chem. Commun.* **2014**, *50*, 9650-9652.
- 41 United Nations Globally Harmonized System of Classification and Labelling of chemicals, fifth edition, **2013**.
- 42 Regulation (EC) No 1272/2008 on the classification, labelling and packaging of substances and mixtures, **2008**.
- 43 Niyogi, S.; Hamon, M. A.; Perea, D. E.; Kang, C. B.; Zhao, B.; Pal, S. K.; Wyant, A. E.; Itkis, M. E.; Haddon, R. C. Ultrasonic dispersions of single-walled carbon nanotubes. *J. Phys. Chem. B* **2003**, *107*, 8799-8804.
- 44 Yau, H. C.; Bayazit, M. K.; Steinke, J. H. G.; Shaffer, M. S. P. Sonochemical degradation of N-methylpyrrolidone and its influence on single walled carbon nanotube dispersion. *Chem. Commun.* **2015**, *51*, 16621-16624.
- 45 Lotya, M.; King, P. J.; Khan, U.; De, S.; Coleman, J. N. High-concentration, surfactant-stabilized graphene dispersions. *ACS Nano* **2010**, *4*, 3155-3162.
- 46 Chabot, V.; Kim, B.; Sloper, B.; Tzoganakis, C.; Yu, A. High yield production and purification of few layer graphene by gum arabic assisted physical sonication. *Sci. Rep.* **2013**, *3*, 1378.
- 47 Zhao, B.; Itkis, M. E.; Niyogi, S.; Hu, H.; Perea, D. E.; Haddon, R. C. Extinction Coefficients and Purity of Single-Walled Carbon Nanotubes. *J. Nanosci. Nanotechnol.* **2004**, *4*, 995-1004.
- 48 Zhao, B.; Itkis, M.E.; Niyogi, S.; Hu, H.; Zhang, J.; Haddon, R. C. Study of the extinction coefficients of single-walled carbon nanotubes and related carbon materials. *J. Phys. Chem. B* **2004**, *108*, 8136-8141.
- 49 Xiong, B.; Cheng, J.; Qiao, Y.; Zhou, R.; He, Y.; Yeung, E. S. Separation of nanorods by density gradient centrifugation. *J. Chromatogr. A* **2011**, *1218*, 3823-3829.
- 50 Chen, S.; Bao, P.; Xiao, L.; Wang, G. Large-scale and low cost synthesis of graphene as high capacity anode materials for lithium-ion batteries. *Carbon* **2013**, *64*, 158-169.
- 51 Gani, R.; Jiménez-González, C.; Constable, D. J. C. Method for selection of solvents for promotion of organic reactions. *Comput. Chem. Eng.* **2005**, *29*, 1661-1676.
- 52 Duereh, A.; Sato, Y.; Smith, R. L. Replacement of Hazardous Chemicals Used in Engineering Plastics with Safe and Renewable Hydrogen-Bond Donor and Acceptor Solvent-Pair Mixtures. *Sustainable Chem. Eng.* **2015**, *3*, 1881-1889.
- 53 Meyer, J. C.; Geim, A. K.; Katsnelson, M. I.; Novoselov, K. S.; Booth, T. J.; Roth, J. S. The structure of suspended graphene sheets. *Nature* **2007**, *446*, 60-63.
- 54 Gonell, S.; Poyatos, M.; Peris, M. High-concentration graphene dispersions with minimal stabilizer: a scaffold for enzyme immobilization for glucose oxidation. *Chem. Eur. J.* **2014**, *20*, 5752-5761.
- 55 Lotya, M.; Hernandez, Y.; King, P. J.; Smith, R. J.; Nicolosi, V.; Karlsson, L. S.; Blighe, F. M.; De, S.; Wang, Z.; McGovern, I. T.; Duesberg, G. S.; Coleman, J. N. Liquid phase production of graphene by exfoliation of graphite in surfactant/water solutions. *J. Am. Chem. Soc.* **2009**, *131*, 3611-3620.
- 56 Malard, L. M.; Pimenta, M. A.; Dresselhaus, G.; Dresselhaus, M. S. Raman spectroscopy in graphene. *Phys. Rep.* **2009**, *473*, 51-87.
- 57 Cançado, L. G.; Jorio, A.; Martins Ferreira, E. H.; Stavale, F.; Achete, C. A.; Capaz, R. B.; Moutinho, M. V. O.; Lombardo, A.; Kulmala, T. S.; Ferrari, A. C. Quantifying defects in graphene via raman spectroscopy at different excitation energies. *Nano Lett.* **2011**, *11*, 3190-3196.
- 58 Cançado, L. G.; Takai, K.; Enoki, T.; Endo, M.; Kim, Y. A.; Mizusaki, H.; Jorio, A.; Coelho, L. N.; Magalhães-Paniago, R.; Pimenta, M. A. General equation for the determination of the crystallite size of nanographite by Raman spectroscopy. *Appl. Phys. Lett.* **2006**, *88*, 163106.
- 59 Assia, O.; Hakim, D. Propagation of Ultrasonic Waves in Viscous Fluids. In *Wave Propagation in Materials for Modern Applications*; Petrin, A., Eds.; InTech: Vienna, **2010**; pp 293-306.
- 60 Chen, I. W. P.; Huang, C. -Y.; Jhou, S. -H. S.; Zhang, Y. -W. Exfoliation and performance properties of non-oxidized graphene in water. *Sci. Rep.* **2014**, *4*, 3928.
- 61 Coleman, J. N. Liquid exfoliation of defect-free graphene. *Acc. Chem. Res.* **2013**, *46*, 14-22.
- 62 Paton, K. R.; Varrla, E.; Backes, C.; Smith, R. J.; Khan, U.; O'Neill, A.; Boland, C.; Lotya, M.; Istrate, O. M.; King, P.; Higgins, T.; Barwich, S.; May, P.; Puczkarski, P.; Ahmed, I.; Moebius, M.; Pettersson, H.; Long, E.; Coelho, J.; O'Brien, S. E. et al. Scalable production of large quantities of defect-free few-layer graphene by shear exfoliation in liquids. *Nat. Mater.* **2014**, *13*, 624-630.

Supporting Information

Identification of High Performance Solvents for the Sustainable Processing of Graphene

Horacio J. Salavagione¹, James Sherwood², Mario De bruyn², Vitaliy L. Budarin², Gary Ellis¹, James H. Clark^{2*}, Peter S. Shuttleworth^{1*}

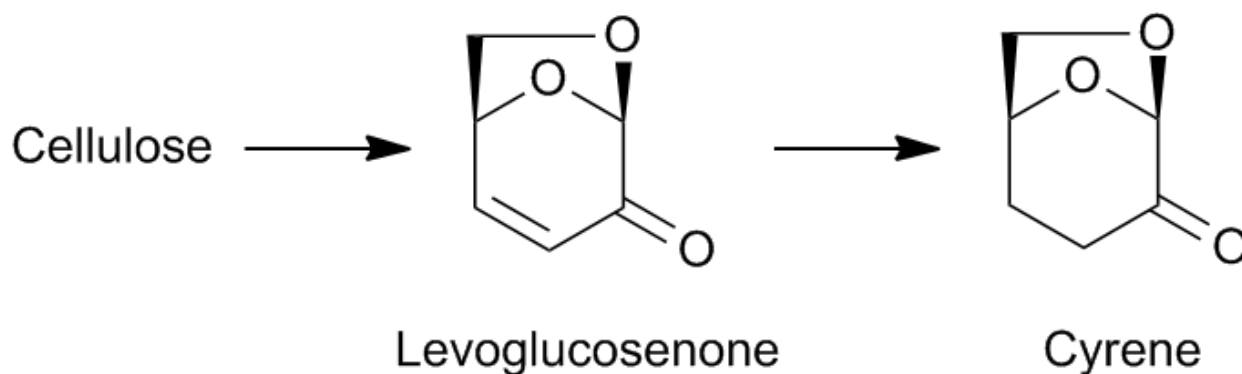
¹ Departamento de Física de Polímeros, Elastómeros y Aplicaciones Energéticas, Instituto de Ciencia y Tecnología de Polímeros, CSIC, c/ Juan de la Cierva, 3, 28006, Madrid (Spain).

² Green Chemistry Centre of Excellence, University of York, Heslington, York, Yorkshire, YO10 5DD (UK).

e-mail: peter@ictp.csic.es

Experimental

Materials. Graphite powder with a particle size of 45 μm was purchased from Aldrich (<45 micron, 99.99%, B.N. 496596-113.4G). CVD-graphene on Si covered with a SiO_2 layer of 90 nm was purchased from Graphenea, Spain. Triacetin and *N*-methyl-2-pyrrolidinone (NMP) were purchased from Sigma Aldrich. Dihydrolevoglucosenone (Cyrene) was obtained from Circa Group Pty Ltd, and later further purified by first passing the solvent through an alumina column and afterwards by vacuum distillation. The synthesis of Cyrene from cellulose *via* levoglucosenone has been previously reported (see Scheme 1).^{1,2}



Scheme S1: Route of dihydrolevoglucosenone (Cyrene) production from cellulose via levoglucosenone.

All other materials were used as received.

Graphene solvent dispersion. The experimental procedure to disperse graphene was as follows: 3 mL of solvent was added to a vial containing ~ 4.5 mg of graphite (Aldrich, <45 micron, 99.99%, B.N. 496596-113.4G). The mixture was treated with an ultrasonic probe (UP400S ultrasonic processor, Hielscher) during 15 minutes and the resulting dispersions

were centrifuged at 7000 rpm for 10 minutes. The supernatant after centrifugation was transferred to a new vial by pipette.

Solvent dispersion concentration. UV-Vis absorption spectra of dispersed graphene in the solvents NMP, Cyrene, and triacetin were recorded on a Perkin Elmer Lambda 35 spectrophotometer and analysed using the dedicated Perkin Elmer UV Winlab v. 2.85.04 software, with the absorption spectrum shown in Figure S1.

For the UV calibration, 1 mL of centrifuged sample of graphene in Cyrene was passed through a fluoroporeTM membrane (0.2 μm pore size) and the solid residue carefully weighed, accounting for any residual solvent to determine the actual dispersion of graphene. The same solution was diluted several times in order to prepare samples with different graphene concentrations. Using the UV absorbance at 660 nm,³ where the spectra of the NMP and Cyrene dispersions both have a gradient of approximately zero, the observed magnitudes of absorbance were recorded. The variation of absorbance divided by cell length, as a function of the concentration of graphene dispersed in the reference solutions of Cyrene were plotted (see Figure 1c, main text) and the line of best fit used to calculate the molar absorptivity coefficient according to the Lambert-Beer law.

Contact angle. A computer controlled microscope Intel QX3 was used to measure the contact angle of the tested solvents. CVD-Graphene (on Si/SiO₂) pieces (Graphenea),⁴ were placed on a manually controlled tilt table with a white light source to illuminate the sample from behind. With the microscope in the horizontal position, the shape of the static drops of the different solvents (3 μL) on the surface using a 60x objective were recorded at room temperature and pressure, and the contact angles calculated using a conventional drop shape analysis technique (Attension Theta optical tensiometer). Please also refer to Figure S3.

Solvent polarity. The calculation of Hansen solubility parameters and Hansen radii was performed with the HSPiP software package (4th Edition 4.1.04, developed by Abbott, Hansen and Yamamoto).

High resolution transmission electron microscopy (TEM). Both Cyrene and NMP dispersions were analysed using two types of TEM at the Centro Nacional de Microscopía Electrónica, Madrid, Spain with the aid of a technician, with TEM micrographs taken at random locations across the grids, to ensure a non-biased assessment. For measurement of graphene flake lateral dimensions, High-resolution HRTEM micrographs were performed on a JEOL JEM-2100 instrument (JEOL Ltd., Akishima, Tokyo, Japan), using a LaB6 filament, a lattice resolution of 0.25 nm and an acceleration voltage of 200 kV. For analysis of the graphene flake layers and molecular integrity of the graphene flakes, measurements were carried out on a High-resolution HRTEM micrographs were performed on a JEOL JEM-3000F instrument (JEOL Ltd., Akishima, Tokyo, Japan), using a LaB6 filament, a lattice resolution of 0.17 nm and an acceleration voltage of 300 kV. Directly after sonication and centrifugation the dispersion was added to an equal volume of acetone to dilute it as it was found that it was too concentrated to achieve a good TEM image, and secondly to aid evaporation of the solvent. Samples were prepared by drop-casting a few millilitres of dispersion onto holey carbon films (copper grids) and dried at 120 °C under vacuum for 12 hours.

Raman spectroscopy characterisation. Raman measurements were undertaken in the Raman Microspectroscopy Laboratory of the Characterisation Service in the Institute of Polymer Science & Technology, CSIC using a Renishaw InVia-Reflex Raman system (Renishaw plc, Wotton-under-Edge, UK), which employed a grating spectrometer with a Peltier-cooled CCD detector coupled to a confocal microscope. The Raman scattering was excited with an argon ion laser ($\lambda = 514.5$ nm), focusing on the sample with a 100x

microscope objective (NA=0.85) with a laser power of approximately 2 mW at the sample. Spectra were recorded in the range between 1000 and 3200 cm^{-1} . All spectral data was processed with Renishaw WiRE 3.2 software. We would like to thank Ms. Isabel Muñoz Ochando from the Instituto de Ciencia y Tecnología de Polímeros de Madrid (ICTP), CSIC for help testing the samples.

Additional results

UV-vis dispersion analysis. The procedure for the preliminary analysis of the graphene dispersion with UV-vis spectroscopy is explained in the Methods section previously. The analysis permitting the calculation of graphene concentration is shown in Figure S1. The UV absorbance spectra are featureless above 500 nm (Cyrene starts to absorb below this value), but due to increased scattering caused by dispersed graphene particles in the case of Cyrene, its baseline is significantly higher than that of NMP and other solvents, indicative of a higher graphene concentration. Photographs of the dispersions immediately after centrifugation and one month later are shown in Figure S2.

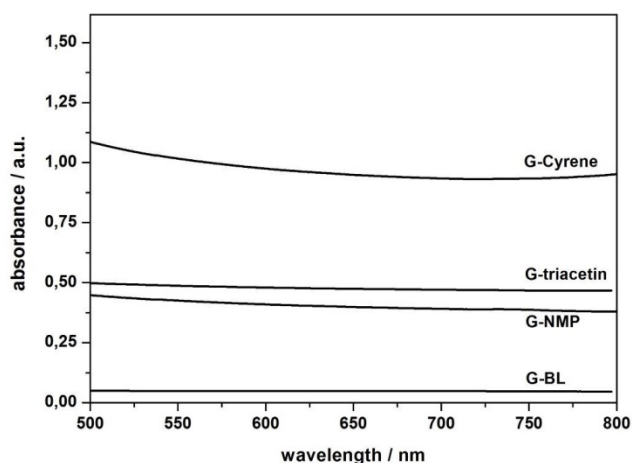


Figure S1. Spectroscopic analysis of graphene dispersion concentrations. The graph shows the UV-visible spectra of graphene dispersions in the solvents Cyrene (G-Cyrene), triacetin (G-triacetin), NMP (G-NMP), and butyl lactate (G-BL).

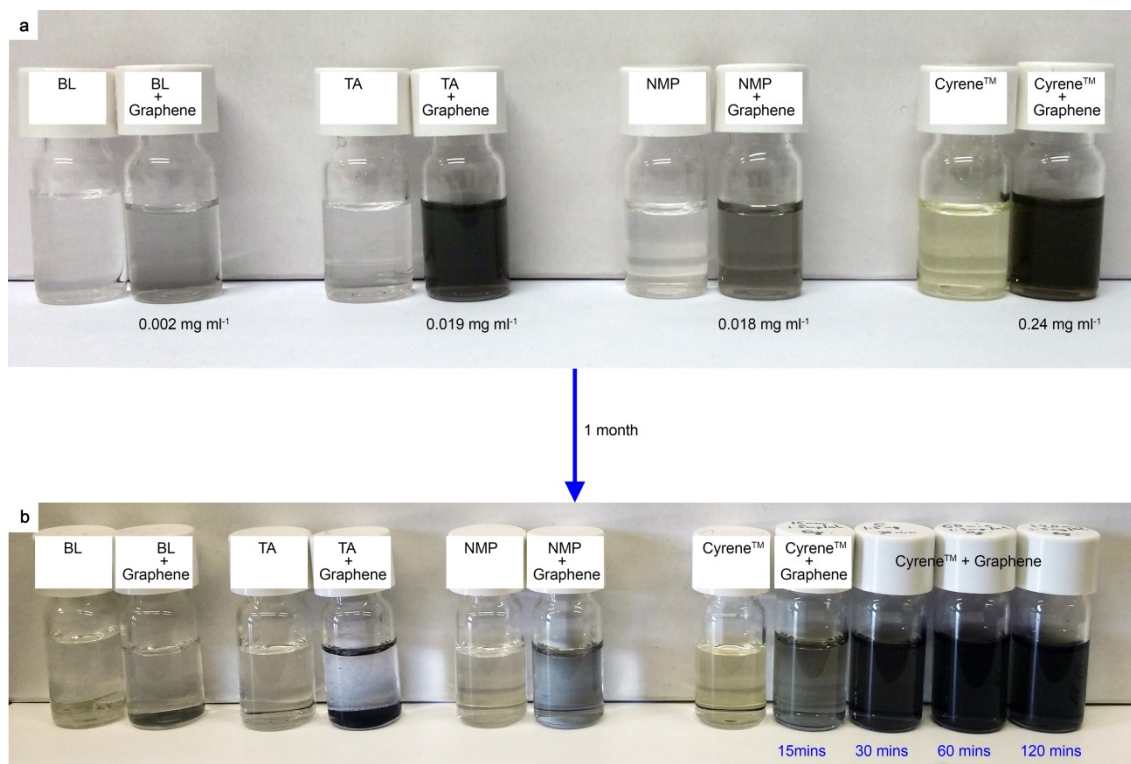


Figure S2. Pictures of the dispersed solvents after sonication and centrifugation. a) Graphene dispersions in butyl lactate (BL), triacetin (TA), *N*-methyl-2-pyrrolidinone (NMP) and Cyrene compared to the original solvent without dispersed graphene. Samples were prepared at an initial concentration of 1.5 mg ml^{-1} , after 15 minutes sonication time followed by two rounds of 7.5 minute centrifugation at 7000 rpm. b) Picture showing the stability of the graphene dispersions after one month, with additional images of Cyrene dispersions after 1 month prepared with various sonication times (same initial concentration of 1.5 mg ml^{-1}).

Surface tension study. The relationship between the contact angles (Figure S3) and the surface energy of the graphene monolayer on Si/SiO₂ can be expressed by Equation 1, which is derived from Young's equation and the work of adhesion of liquids in solid surfaces and applying the Neumann's equation of state theory.⁵ In Equation 1, β is the constant coefficient of graphene.

$$\ln \left[\delta_{sol} \left(\frac{1 + \cos\theta}{2} \right)^2 \right] = -2\beta(\delta_G - \delta_{sol})^2 + \ln(\delta_G) \quad \text{Eq. (1)}$$

A plot of the left-hand side of the Equation 1 as a function of the solvent surface energy (δ_{sol}) was fitted with a second-order polynomial curve, from which β and the surface tension of graphene on SiO₂ can be determined (δ_G). A good fit of the experimental points (excluding triacetin) was obtained (Figure S4).

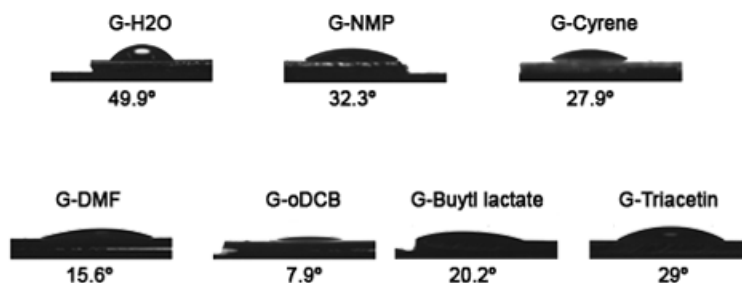


Figure S3. Contact angle study for the verification of graphene affinity on CVD-graphene monolayer on Si/SiO₂.

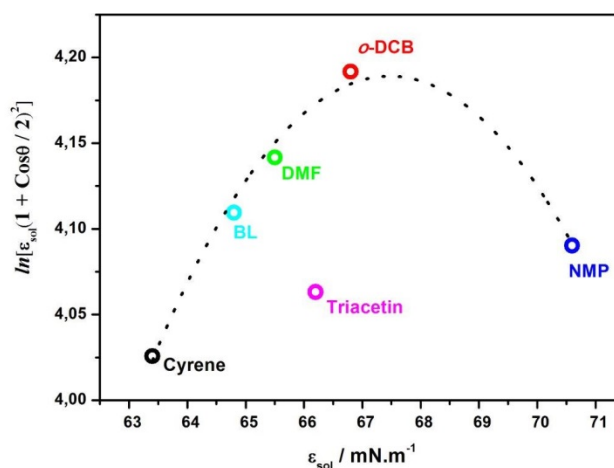


Figure S4. Calculation of the graphene surface energy. Variation of contact angle with solvent's surface energy according to Neumann's equation including triacetin.

High solvent affinity for the graphene surface manifests itself through the wettability of the solvent and a low contact angle.⁵ The tension at this solid-liquid interface is a result of attractive intermolecular forces. If the interfacial tension between the surface and the solvent is low then there will be little enthalpy loss in creating the surface-solvent interface, hence minimizing the energy cost of exfoliation. The lowest contact angles, and subsequently the best wetting performances, are observed for solvents with a surface tension between 35 mN m⁻¹ and 38 mN m⁻¹, corresponding to *o*DCB and DMF. As anticipated from the higher graphene concentration in Cyrene in relation to NMP, the contact angle formed by Cyrene was found to be lower than that for NMP, but only marginally. Considering all the organic solvents, the surface energy value of the graphene employed was calculated to be 67 mN m⁻¹ using Neumann's equation of state theory, in excellent agreement with previous findings.⁶

It has been previously demonstrated that the contact angle of water droplets on graphene depends on the number of layers,^{7,8} the substrate,⁹ and the duration of the experiment, which can be affected through the absorption of airborne contaminants, including hydrocarbons.¹⁰ Although in our study we are also using a range of organic solvents, we have considered these variables. In summary the time dependence is controlled by collecting the contact angle values immediately after depositing the drop of solvent. The thickness and

uniformity of the CVD-graphene were evaluated by Raman spectroscopy. The I_{2D}/I_G intensity ratio and the full width at half-maximum of the 2D band, related to the number of CVD-graphene layers, are 1.7 ± 0.2 and $36.9 \pm 0.8 \text{ cm}^{-1}$ respectively, resembling the values previously observed for CVD-graphene.^{11,12} This data is indicative of graphene uniformly distributed on the Si/SiO₂ surface, allowing us to discard the effect of the graphene thickness on the contact angles. Moreover, reference experiments of contact angles on Si/SiO₂ wafers (without graphene) were conducted to evaluate the influence of the substrate. The measured values were very similar for all organic solvents ($\sim 32.0^\circ$ to 36.6°) demonstrating minimal influence of the Si/SiO₂ substrate on the contact angle.

High resolution transmission electron microscopy. Lower magnification images of the dispersions were taken as an initial assessment of the quality of the graphene flakes, and also aid with the measurement of the lateral flake dimensions. It can be seen in Figure S5, images A and B (Cyrene) that the flakes are much better dispersed in comparison to the flakes seen in images E and F for NMP, which by comparison are much more agglomerated. This is clearer when comparing images in Figure S5 C and D with those in Figure S5 G and H, where the latter are overall larger, but from their representative diffraction patterns are observed to be multilayer to graphitic. The flakes formed in Cyrene are bi- to few layers. Figure S6, images A-D, show HRTEM images of various flakes with well-defined edges, ranging from probable single layer graphene to few layer graphene produced from the Cyrene graphene dispersion. Images E-H are for those obtained from the NMP-graphene dispersion, and as can be seen they range from few layer flakes to graphitic particles in nature. Additionally, when comparing the lateral dimensions of the samples prepared in either Cyrene or NMP it can be seen that for flake sizes with ≤ 10 layers, flakes produced using Cyrene are actually larger on the whole (see Figure S7).

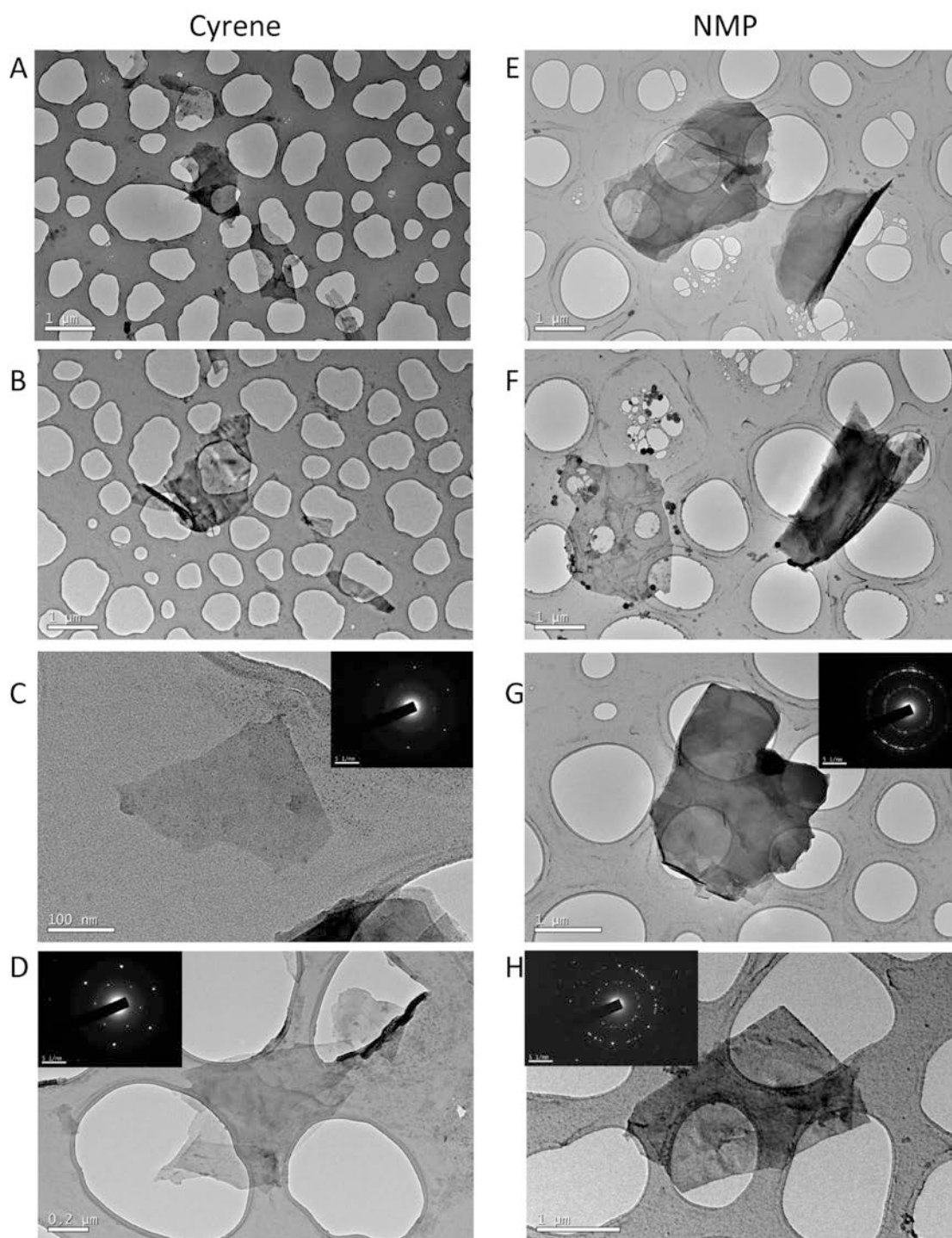


Figure S5. High resolution transmission electron microscopy (HRTEM) of graphene produced in Cyrene and NMP. Lower magnification TEM images of dispersions achieved with Cyrene (inset images A and B) and NMP (E and F). High magnification images of flakes with various layers can be seen in images C and D (Cyrene) and G and H (NMP).

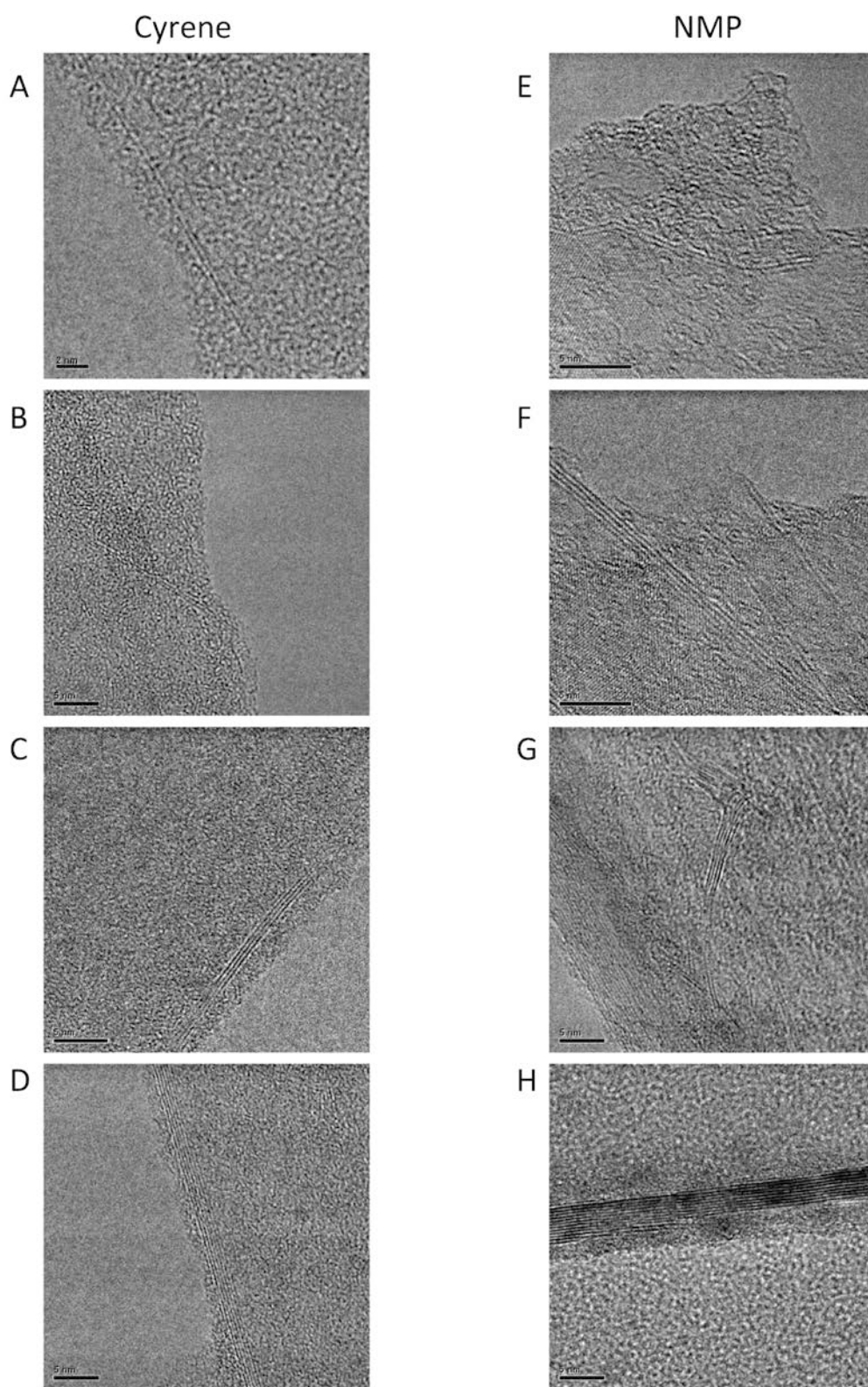


Figure S6. HRTEM images showing the edges of Cyrene dispersed graphene (inset images A-D) and NMP dispersed graphene (E-H).

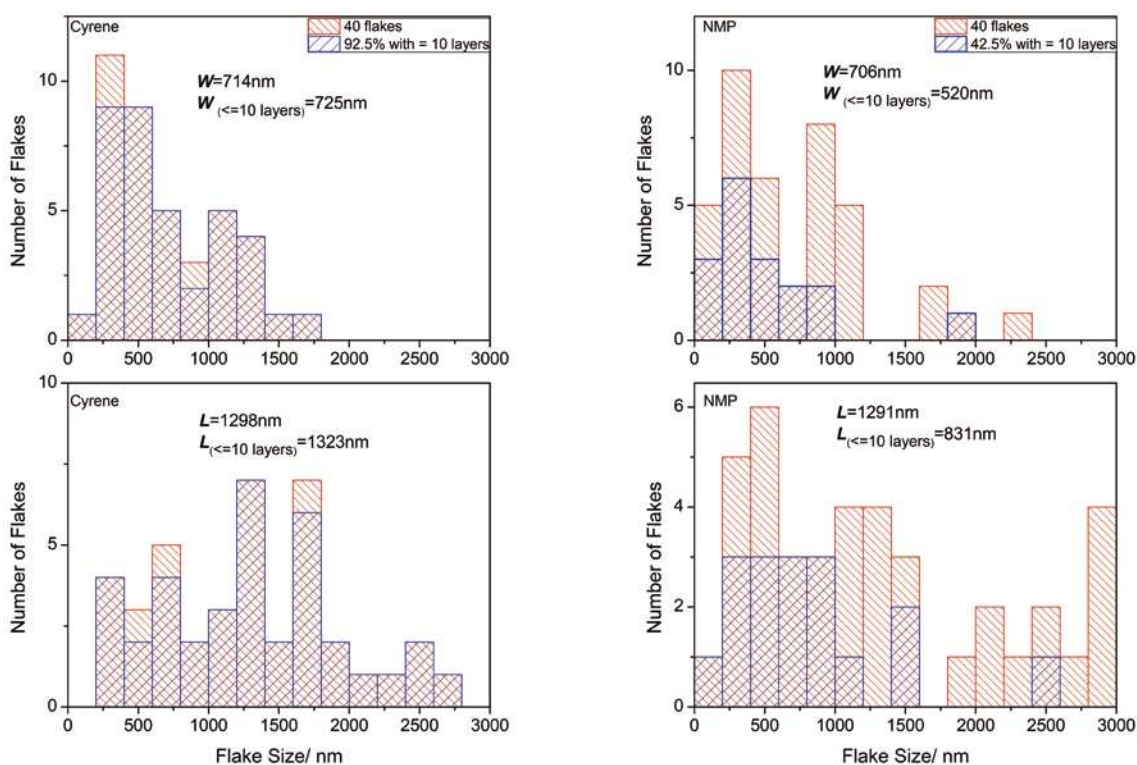


Figure S7. Flake length (L) and width (W) dimensions taken from TEM measurements for both Cyrene (left) and NMP (right) dispersions.

Raman graphene quality analysis. Examination of the Raman 2D band in this work was found to be very instructive in ruling out whether the postulated ‘protection’ offered by viscous solvents counteracts the critical role of surface tension. It is accepted that the number of Lorentzian curves (FWHM ~ 24) making up the 2D band relates to the number of stacked graphene layers.¹³⁻¹⁵ Here deconvolution of 2D Raman band for Cyrene suggested the formation of polydisperse samples ranging from two to a few and multilayers graphene, similar to NMP treated under the same conditions (Figure S8). Furthermore, the 2D band width, another parameter used to determine the thickness of graphene laminates, is very similar for both samples, which also suggests that they represent a similar thickness of graphene.¹⁶ The difference between this and the results of TEM *etc.* are due to the extended drying times of the dispersion on the Si/SiO₂ wafer in comparison to the holey carbon grid used for TEM and also the fact that monolayer graphene is virtually invisible under an optical

microscope to be able to locate them and test them, even when using recommended Si/SiO₂ (300 nm).

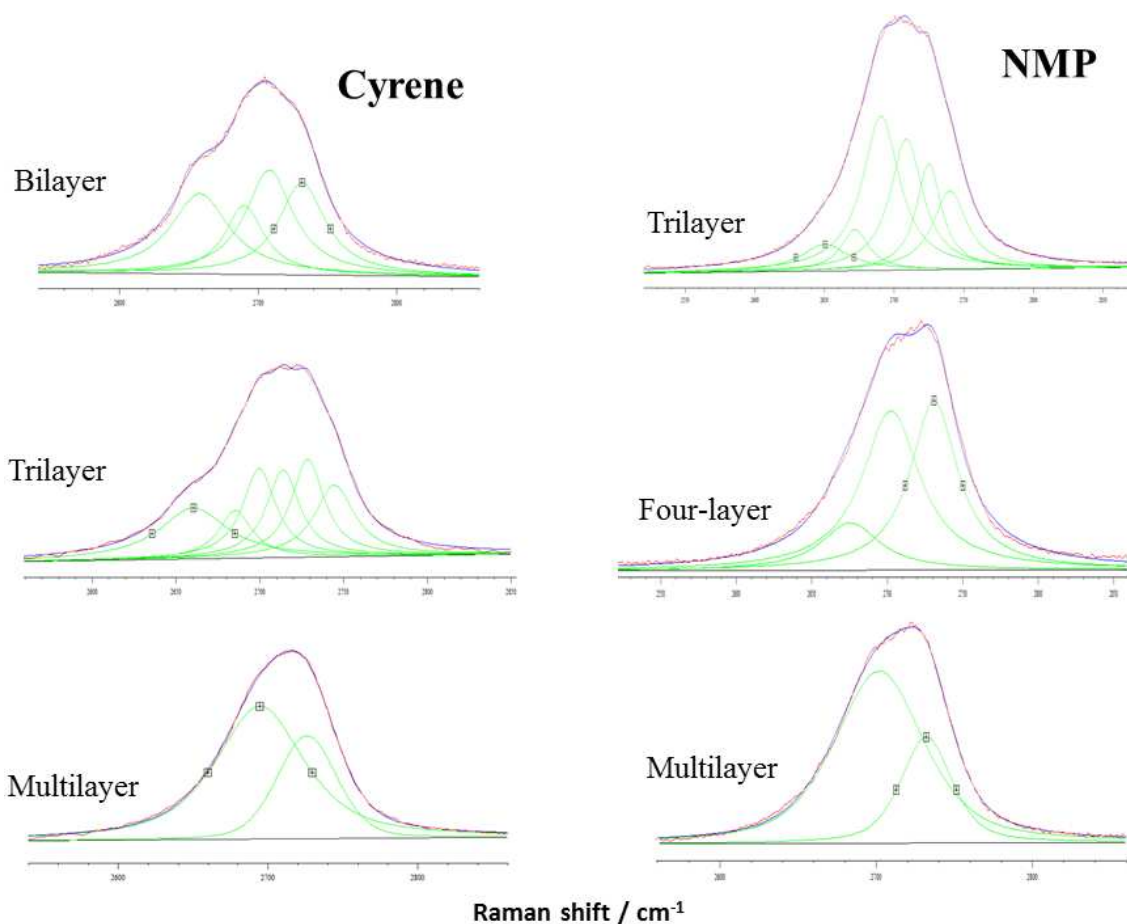


Figure S8. Raman 2D band deconvolution to estimate the number of graphene stacked layers. The spectra were acquired in different points of samples deposited by drop-casting on Si/SiO₂ substrates.

A general expression to estimate the crystallite size L_a from the integrated intensity ratio I_D/I_G has been proposed by Cançado *et al.*,¹⁷ and can be written as follows (Equation 2) where λ is the laser wavelength in nm, in this case 514 nm.

$$L_a(\text{nm}) = 2.4 \times 10^{-10} \lambda_l^4 \left(\frac{I_D}{I_G} \right)^{-1} \quad \text{Eq. (2)}$$

The distance between defects (L_D) and the defect density (n_D) can also be estimated from the I_D/I_G using experimentally determined equations.¹⁸ The L_D can be written as is shown in Equation 3, and the density of defect as Equation 4.

$$L_D^2 (nm^2) = (1.8 \pm 0.5) \times 10^{-9} \lambda_l^4 \left(\frac{I_D}{I_G} \right)^{-1} \quad \text{Eq. (3)}$$

$$n_D (cm^{-2}) = \frac{(1.8 \pm 0.5) \times 10^{22}}{\lambda_l^4} \left(\frac{I_D}{I_G} \right) \quad \text{Eq. (4)}$$

Changes in L_a , L_D , and the defect density (n_D) compared with the viscosity of the tested solvents are shown in Figure S9.

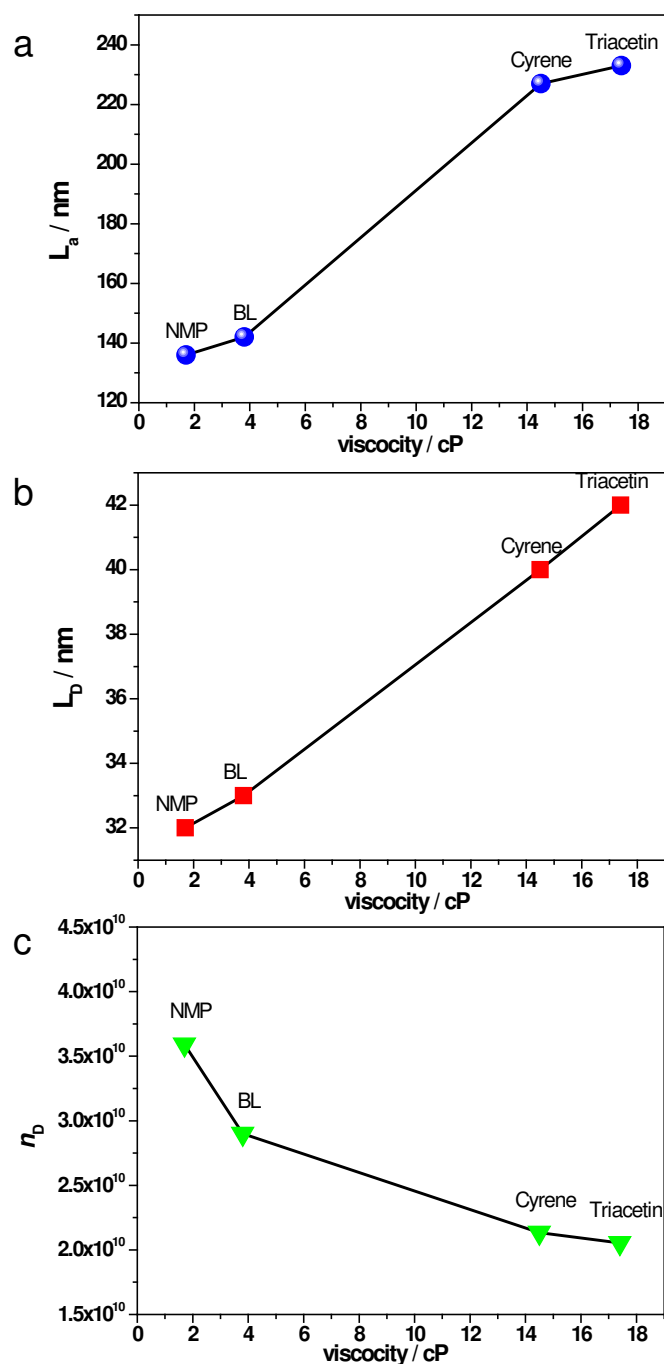


Figure S9. Variation in characteristic parameters of graphene flakes, obtained from the I_D/I_G Raman ratio. A) Crystallite size, L_a ; B) distance between defects (L_D); and, C) the density of defects (n_D). The viscosity of the tested solvents increases in the following order: NMP, Cyrene, and triacetin.

The evaluated parameters display an apparent relationship with solvent viscosity. As expected, the flakes obtained in solvents with higher viscosity display larger graphitic domains and lower density of defects. Although solvents of intermediate viscosity need to be

tested to appropriately obtain an equation describing the variation of each parameter with viscosity, the data in Figure S9 clearly demonstrates the effect of viscosity on the structural integrity of graphene flakes.

Exfoliation optimization. The experimental parameters, e.g. sonication time and initial graphite concentration that determine the concentration of the dispersed graphene were re-evaluated. Long sonication times have previously been reported as a means to obtain high graphene concentrations in NMP.¹⁹ This this may also be advantageous for dispersions in Cyrene. The aim of our investigation here was to establish the optimal conditions that maximize the dispersion of graphene for commercially pertinent applications, whilst preserving the structural integrity of the graphene flakes.

Firstly, different initial concentrations of graphite, C_i , of 0.5, 1.5, 5.0 and 10 mg mL⁻¹ were tested to evaluate the exfoliation of graphite to dispersed graphene in Cyrene (Figure S10a). The amount of dispersed material was determined by UV-visible spectroscopy, where the absorbance at 660 nm was measured in the same way as previously outlined. An almost linear dependence of the amount of dispersed graphene versus the starting graphite amount was observed up to $C_i = 5$ mg mL⁻¹, with the gradient accounting for an additional 0.15 mg of dispersed particles for every 1 mg increase in the starting graphite loading. Few gains are made beyond an initial graphite concentration of 5 mg mL⁻¹, but still graphene concentrations of ~1 mg mL⁻¹ can be reached with an initial graphite load of $C_i = 10$ mg mL⁻¹. Figure S10b presents the percentage of the initial graphite that can be converted into dispersed particles. It is evident that this quantity initially increases, reaching a maximum (16%) in the range 1.5 mg mL⁻¹ < C_i < 5 mg mL⁻¹ and then decreases significantly to no more than 10% when $C_i = 10$ mg mL⁻¹. This trend can be related to the effect of powdered graphite particles on the efficiency of sonication, and consequently exfoliation. Specifically, high amounts of

suspended graphite powder minimize the efficiency of the ultrasound irradiation leading to less particles being able to benefit from the desired cavitation phenomenon.²⁰

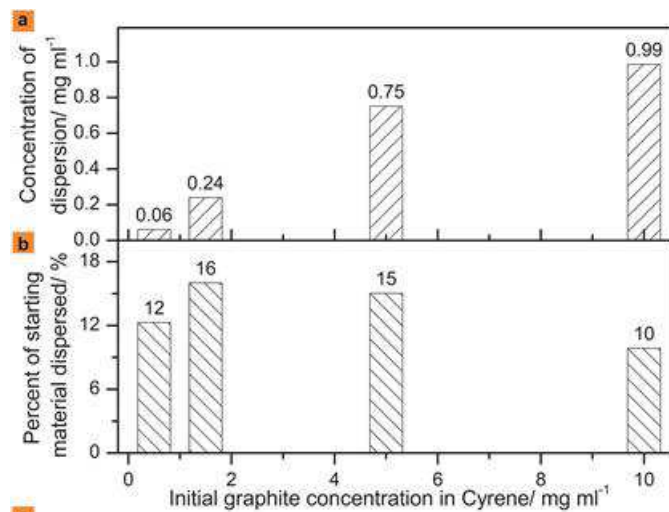


Figure S10. Graphene dispersion parameter optimization. a) Variation of the initial graphite concentration versus the measured the concentration of graphene dispersed after the standard 15 minutes sonication and 10 minutes centrifugation, and, b) the respective percentage of starting graphite that in-turn converts to dispersed graphene.

Solvent selection procedure

Overview. A solvent selection protocol was developed to identify ideal solvents for graphene processing and to help define the precise role of the solvent. Given the clearly recognisable need, the methodology was developed to find a high performance yet green solvent. Algorithms for solvent selection have been used previously to optimise the solvent for simple extractions, and in examples of reaction chemistry.²¹ If the requirements of the solvent can be defined in terms of measurable properties, then we postulated that the principle can also be applied to the more complex problem of graphite exfoliation and the subsequent dispersion of graphene flakes in solution. There has been much debate over the exact role of the solvent in the processing of carbon nanostructures,²²⁻²⁵ which is not fully understood. Nevertheless there is a consensus that solvent surface energy and viscosity are both crucially important in order to achieve an acceptable concentration of dispersed graphene.^{3,25} The polarity of the medium is also influential, and Hansen solubility parameters have been used previously to correlate graphene concentration to solvent polarity.^{26,27} However different reports do not always agree on the significance of each solvent property, or in some instances what the ideal value of that property actually is.^{3,5} That being the case, an approach to solvent selection that can be easily updated, added to, or otherwise modified is greatly beneficial.

Here we report a high throughput screening of a large database of solvents in order to identify green solvents able to disperse graphene in relatively high concentrations. After a comprehensive selection process, the most promising solvent candidates, as indicated through calculation, were subjected to an experimental validation of their performance. This multi-stage assessment of solvent properties was designed to refine a large solvent dataset, far beyond the number of solvents that could actually be tested experimentally, to only the environmentally friendly solvent candidates with an anticipated high performance. This is a

key difference between this approach and the solely experimental methods of other studies that make use of Hansen solubility parameters.²⁶ A series of experiments and analysis confirmed the theoretical predictions, with Cyrene for example achieving highly concentrated dispersions of quality graphene flakes.

To the best of the authors' knowledge, this work is the first attempt to select a solvent for creating graphene dispersions by considering relevant properties in a logical, systematic way, but crucially without the restriction of choosing a solvent from a small experimental set. The approach employed reduces a large number of possible solvent candidates to a shortlist consisting of only those solvents that meet the requirements of each criterion. Thus, experimental validation of the solvent selection protocol is only required for a minimal number of solvents, thus creating a streamlined investigation that at the same time actually encompasses several hundreds of solvents more than a typical, experimentally led project. The act of carrying out the solvent selection process creates a better understanding of the relevant solvent characteristics. This in turn assists with future solvent development, where the solvent selection process may be adapted or new solvent candidates introduced in later iterations. A concise version of the assessment is provided as a separate (Microsoft Excel) file.

The first round of the methodology concerns the solvent properties that influence the performance of the process (*i.e.* ultrasound assisted exfoliation and graphene dispersion). A polarity matching exercise using Hansen solubility parameters established suitable solvents on the basis of bulk solution interactions with graphene. Target parameters representing the polarity of graphene were obtained from the literature.²⁶ Secondly the interaction between the solvent and graphene through their surface energies, again relevant to exfoliation and dispersion stability, was also used to select promising solvent candidates.^{5,6} Finally the stability of a graphene suspension was approximated using Stokes' law of settling velocities,

where the density/viscosity ratio is important (as explained subsequently). The three criteria were applied in individual assessments, not sequentially (Table S1). This is so that if a requirement is changed, the recalculation of the solvent shortlist is simplified. Solvent candidates move through to the next stage of the assessment only if they meet the requirements of all three parallel performance criteria.

Table S1. Solvent selection performance criteria.

Performance metric	Measurement	Target	Requirement
Solvent-solute interaction	Polarity (calculated)	$\delta_D = 18 \text{ MPa}^{0.5}$ $\delta_P = 9.3 \text{ MPa}^{0.5}$ $\delta_H = 7.7 \text{ MPa}^{0.5}$	Hansen distance between target and solvent lower than $6.5 \text{ MPa}^{0.5}$.
Solvent-solute interaction	Surface tension	$\gamma = 38.2 \pm 6$ $\text{mN}\cdot\text{m}^{-1}$	Solvent surface tension falls within designated range.
Dispersion stability	Density ($\rho / \text{g}\cdot\text{mL}^{-1}$) and dynamic viscosity ($\mu / \text{g}\cdot\text{s}^{-1}\cdot\text{m}^{-1}$)	$\rho/\mu \leq 1.20 \cdot 10^6$ $\text{s}\cdot\text{m}^{-2}$	Low density/viscosity ratio.

The original dataset of solvents exceeded 10,000 entries. The large number of solvent candidates was processed using the HSPiP solubility estimation software package, sorting by polarity. The remaining data analysis was performed in a spreadsheet (refer to the separate electronic supplementary information file). Many of the solvents contained in the dataset lack experimental viscosity and surface tension data, meaning they cannot pass all the solvent selection criteria for this reason alone. However this exercise does highlight promising solvents that could be synthesised and their additional physical properties tested. Computational estimates could also guide this task and future work will investigate this possibility further. The original HSPiP dataset from which the list of solvent candidates was derived was supplemented by a number of bio-based solvents, to which special interest was

paid within the assessment (Table S2). A summary of how each bio-based solvent fared during the solvent selection process is maintained throughout the following discussions.

Table S2. Bio-based solvents included in the solvent selection process.

Solvent name	Bio-based content*	Source[§]
1,2-Pentanediol	100%	Pyrolysis of carbohydrate
1,2-Propanediol	100%	Derived from glycerol
1,3-Propanediol	100%	Derived from glycerol
1,4-Butanediol	100%	Fermentation product
1-Butanol	100%	Fermentation product
2-Butanol	100%	Fermentation product
2-Methyltetrahydrofuran	100%	Pyrolysis of carbohydrate
2-Octanol	100%	Synthesised from vegetable oils
2-Propanol	100%	Fermentation product
Acetic acid	100%	Fermentation product
Acetone	100%	Fermentation product
Acetyltributyl citrate	18%	Made from citric acid
Butyl lactate	43%	Made from lactic acid
Butyric acid	100%	Fermentation product
Cyrene	100%	Pyrolysis of carbohydrate

Table S2. Bio-based solvents included in the solvent selection process. (continued).

Solvent name	Bio-based content*	Source[§]
Diethoxymethane	80%	Made with bio-ethanol
Dimethyl ether	100%	Made from bio-gas
Dimethyl isosorbide	75%	Pyrolysis of carbohydrate
Dimethyl sulphoxide	100%	Made from dimethyl sulphide
<i>d</i> -Limonene	100%	Essential oils

Ethanol	100%	Fermentation product
Ethyl acetate	100%	Made from bio-ethanol
Ethyl lactate	100%	Made from lactic acid
Ethylene glycol	100%	Made from bio-ethanol
Eugenol	100%	Essential oils
Furfural	100%	Pyrolysis of carbohydrate
Furfuryl alcohol	100%	Pyrolysis of carbohydrate
Glycerol	100%	Vegetable oils
Glycerol carbonate	75%	Derived from glycerol
Glycerol formal	75%	Derived from glycerol
Isoamyl alcohol	100%	Fermentation product
Isobutanol	100%	Fermentation product
Isoeugenol	100%	Essential oils
Lactic acid	100%	Fermentation product
Lauric acid	100%	Vegetable oils
Levulinic acid	100%	Pyrolysis of carbohydrate
Methanol	100%	Made from bio-gas
Methyl lactate	75%	Made from lactic acid
Methyl oleate	95%	Synthesised from vegetable oils

Table S2. Bio-based solvents included in the solvent selection process. (continued).

Solvent name	Bio-based content*	Source [§]
Oleic acid	100%	Vegetable oils
<i>p</i> -Cymene	100%	Made from limonene
Solketal	50%	Derived from glycerol
<i>t</i> -Butyl ethyl ether	33%	Made with bio-ethanol
Tetrahydrofuran	100%	Pyrolysis of carbohydrate
Tetrahydrofurfuryl alcohol	100%	Pyrolysis of carbohydrate

Triacetin	33%	Derived from glycerol
Triethyl citrate	100%	Made from citric acid
α -Pinene	100%	Essential oils
α -Terpineol	100%	Essential oils
β -Pinene	200%	Essential oils
γ -Valerolactone	100%	Pyrolysis of carbohydrate

**Bio-based content is calculated on the basis of the number of carbon atoms from biomass origin as a percentage of the total carbon content.*

§*References are provided in the supplementary excel file.*

The second phase of the solvent selection process rejects solvents with obvious environmental, health and safety (EHS) issues under scrutiny by legislation. The first of these requirements is that no solvent possesses known carcinogen, mutagen, or reprotoxic (CMR) characteristics. This is supplemented with an acute toxicity assessment, for these solvents should also be avoided where possible (Table S3). Then the environmental persistency, bioaccumulation, and toxicity (PBT) of solvents meeting the performance criteria was considered. These health and environmental requirements are implemented in the solvent selection process according to the requirements of the EU regulation (EC) No 1907/2006, Registration, Evaluation, Authorisation & restriction of CHemicals (REACH) and the EU regulation (EC) No 1272/2008, Classification, Labelling and Packaging (CLP). It is important to align the requirements of each criteria to formal legislated property values in order to be industrially and commercially relevant. Arbitrary thresholds have been avoided so not to introduce a preference or inadvertent bias for a particular solvent.

Table S3. Solvent selection legislative criteria.

EHS metric	Indicator	Requirement
		<i>CMR or acutely toxic</i>

Acute toxicity	H300, H301, H310, H311, H330, or H331 hazard statements*	LD ₅₀ >300 mg/kg (avoiding CLP category 1, 2, or 3: fatal/toxic).
Carcinogenic	Carcinogenicity category 1A, 1B, or 2*	Neither a category 1 or 2 carcinogen (REACH).
Mutagenic	Germ cell mutagenicity categories 1A, 1B, or 2*	No evidence of mutagenicity (REACH), including animal trials and Ames test.
Reproductive toxin	Reproductive toxicity categories 1A, 1B, or 2*	Neither a category 1 or 2 reproductive toxicant (REACH).

PBT**

Persistent	Biodegradation (multiple test methods and calculations available).	Solvent must be considered as biodegradable.
Bioaccumulating	logP	logP < 4 indicates potential to bioaccumulate (CLP).
Toxic	EC ₅₀	EC ₁₀ > 0.01 mg/L (REACH).

*The associated hazard statements are defined in the EU CLP directive (Regulation No. 1272/2008).

**All three categories must apply for a substance to be considered PBT, but for this assessment each category is considered individually.

Solvent candidates meeting the performance criteria and also found to have suitable EHS profiles formed a final shortlist, and were then ranked according to additional criteria describing the greenness of each solvent. The topic of greenness is highly subjective, and this is an undesirable approach when making an assessment. Therefore solvents were just compared in this respect, and not selected or rejected on the basis of any green chemistry principles. Indicators of greenness were chosen that could be discussed and compared in the context of regulation (Table S4). No thresholds were set, although ideal target values derived from legislation are suggested to help identify the most promising of candidates. European regulation (EC) 1272/2008 on classification, labelling and packaging of substances and mixtures (CLP) and European Directive 2010/75/EU (industrial emissions directive) are both helpful in this respect. The toxicity threshold values are larger than what were used in the

EHS criteria, broadened out to include less severe hazards, yet still requiring labelling according to the CLP directive. In addition, bio-based solvents made from renewable resources were prioritised, under the guidance of European Technical Specification TS/16766.²⁸ This process helped to identify butyl lactate, Cyrene, and triacetin as the primary candidates for the sustainable solvent processing of graphene, incorporating practical, regulatory, environmental, health, and safety aspects as part of this judgement. Greater detail on each of these assessment phases is now provided. A spreadsheet containing the solvent selection calculations has also been made available for greater detail.

Table S4. Solvent selection greenness criteria.

Greenness criteria	Target or threshold value	Justification and context
<i>Renewability</i>		
Bio-based content	≥25%	Minimum of 25% bio-based carbon content (as proportion of total carbon content) given in European technical specification TS/16766, entitled <i>Bio-based solvents: Requirements and test methods</i> to qualify as a bio-based product.
<i>Toxicity</i>		
LD ₅₀ (rat, oral)	> 2000 mg·kg ⁻¹	'Acute toxicity' threshold, below which a substance is recognised as harmful (European regulation (EC) 1272/2008, CLP).
<i>Flammability</i>		
Autoignition temperature	None set.	Indicative of safety. No threshold listed in the CLP regulation.
Flash point	> 60 °C	'Flammable liquids' threshold (CLP).
<i>Environmental impact</i>		
Vapour pressure	< 0.075 mmHg	Industrial emissions 'VOC' threshold (European directive 2010/75/EU).
logP	< 4	'Harmful to the aquatic environment' threshold (CLP), applied in combination with EC ₅₀ .
EC ₅₀ (Daphnia magna, 48 hours)	> 100 mg·L ⁻¹	'Harmful to the aquatic environment' threshold (CLP), applied in combination with logP.
Biodegradability	None set.	Indicative of persistence.

Hansen solubility. The Hansen solubility parameters were originally established as an empirical description of polymer solubility.²⁹ However they are now widely used to identify solvents for a wide range of solutes, including carbon nanostructures.^{5,30-32} In Hansen solubility theory, solutes are predicted to be most soluble in solvents with a similar polarity, as defined by three scales describing dispersion forces (δ_D), dipole forces (δ_P), and hydrogen

bonding interactions (δ_H). The length of a vector connecting a solvent to a solute in this three dimensional Hansen space is indicative of the likely solubility. Using characteristic values for graphene ($\delta_D \sim 18.0 \text{ MPa}^{1/2}$; $\delta_P \sim 9.3 \text{ MPa}^{1/2}$; $\delta_H \sim 7.7 \text{ MPa}^{1/2}$),²⁶ potential solvents can be found computationally. The Hansen parameters are typically calculated rather than obtained from experiments, so the potential solvent set is infinite. This equally applies to theoretical solvent structures before they are first synthesised. Using the *Hansen Solubility Parameters in Practice* (HSPiP) software, a number of potential graphene dispersing solvents were identified from more than 10,000 candidates contained within the software. As stated earlier, this dataset was complimented with 51 bio-based solvent entries taken from the University of York's *Sustainable Solvent Selection Service* (S4) database.

A representative selection of solvents is shown in the following polarity diagram to demonstrate the solvent selection process (Figure S11). The assignment of solvents and non-solvents, and hence the boundary of the so-called solubility sphere (shown in green) was defined using a minimal number of experimental observations already available in the literature. While acetone is seen as a poor solvent for graphene dispersibility,²⁶ it is actually a better polarity match to graphene in the 3D Hansen space (radius of $5.2 \text{ MPa}^{0.5}$) than DMF ($5.8 \text{ MPa}^{0.5}$), the latter being a recognised solvent. This suggests other solvent properties are relevant. A sphere radius of $6.5 \text{ MPa}^{0.5}$ was chosen to differentiate between potentially suitable and unsuitable solvents on the basis of polarity (Figure S11). Acetone and DMF are both contained within this boundary.

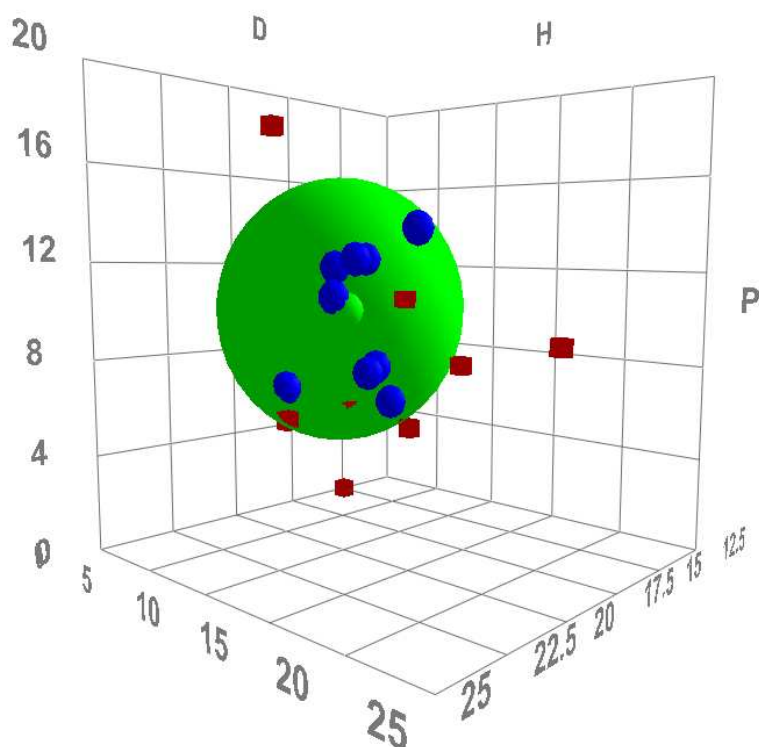


Figure S11. A three dimensional Hansen solubility map, where graphene is shown as the green data point, some representative solvents as solid blue data points, and a selection of non-solvents shown as red data points. The green sphere marks the boundary between solvents and non-solvents as calculated by the HSPiP software.

From this analysis a great number of solvent candidates can be ruled out because of their unsuitable polarity. From the original solvent set, more than 4000 compounds were identified as having a desirable polarity, and retained for further consideration. Note that the other two performance criteria rely on experimental data (*i.e.* density/viscosity and surface tension), and so a great deal of the solvents identified on the basis of their polarity cannot continue onwards through the solvent selection process. However very good polarity matches could always warrant experimental determination of these physical properties in the search for alternative solvents, although this was not pursued at this time.

Most of the 51 bio-based solvents in the original dataset do not possess the desired polarity. Only 18 met this requirement (Table S5), of which the closest polarity match to graphene was Cyrene (dihydrolevoglucosenone), followed by dimethyl isosorbide. Prominent

bio-based solvents with an undesirable polarity, and thus eliminated from the assessment, included limonene, ethanol, and glycerol.

Table S5. Polarity characteristics of the bio-based solvents.

Solvent name	$\delta_D / \text{MPa}^{1/2}$	$\delta_P / \text{MPa}^{1/2}$	$\delta_H / \text{MPa}^{1/2}$	Radius	Status
1,2-Pentanediol	16.7	7.2	16.8	9.69	Fail
1,2-Propanediol	16.8	10.4	21.3	13.9	Fail
1,3-Propanediol	16.8	13.5	23.2	16.2	Fail
1,4-Butanediol	16.6	11.0	20.9	13.6	Fail
1-Butanol	16.0	5.7	15.8	9.72	Fail
2-Butanol	15.8	5.7	14.5	8.86	Fail
2-Methyltetrahydrofuran	16.9	5.0	4.3	5.91	Pass
2-Octanol	16.1	4.2	9.1	6.51	Fail
2-Propanol	15.8	6.1	16.4	10.3	Fail
Acetic acid	14.5	8.0	13.5	9.18	Fail
Acetone	15.5	10.4	7.0	5.17	Pass
Acetyltributyl citrate	16.7	2.5	7.4	7.29	Fail
Butyl lactate	15.8	6.5	10.2	5.78	Pass
Butyric acid	15.7	4.8	12.0	7.74	Fail
Cyrene	18.8	10.6	6.9	2.21	Pass
Diethoxymethane	15.4	5.7	5.1	6.84	Fail

Table S5. Polarity characteristics of the bio-based solvents. (continued).

Solvent name	$\delta_D / \text{MPa}^{1/2}$	$\delta_P / \text{MPa}^{1/2}$	$\delta_H / \text{MPa}^{1/2}$	Radius	Status
Dimethyl isosorbide	17.6	7.1	7.5	2.35	Pass
Dimethyl sulphoxide	18.4	16.4	10.2	7.57	Fail
<i>d</i> -Limonene	17.2	1.8	4.3	8.39	Fail

Ethanol	15.8	8.8	19.4	12.5	Fail
Ethyl acetate	15.8	5.3	7.2	5.97	Pass
Ethyl lactate	16	7.6	12.5	6.48	Pass
Ethylene glycol	17.0	11.0	26.0	18.5	Fail
Eugenol	19.0	7.5	13.0	5.94	Pass
Furfural	18.6	14.9	5.1	6.29	Pass
Furfuryl alcohol	17.4	7.6	15.1	7.69	Fail
Glycerol	17.4	11.3	27.2	19.6	Fail
Glycerol carbonate	17.9	25.5	17.4	18.9	Fail
Glycerol formal	18.4	10.6	16.5	8.93	Fail
Isoamyl alcohol	15.8	5.2	13.3	8.22	Fail
Isobutanol	15.1	5.7	15.9	10.7	Fail
Isoeugenol	18.9	5.7	9.9	4.59	Pass
Lactic acid	17.3	10.1	23.3	15.7	Fail
Lauric acid	16.2	4.1	7.4	6.33	Pass
Levulinic acid	17.1	10.4	13.5	6.17	Pass
Methanol	14.7	12.3	22.3	16.3	Fail
Methyl lactate	16.9	8.3	16.1	8.74	Fail
Methyl oleate	16.2	3.8	4.5	7.31	Fail
Oleic acid	16.0	2.8	6.2	7.78	Fail
<i>p</i> -Cymene	17.3	2.4	2.4	8.81	Fail

Table S5. Polarity characteristics of the bio-based solvents. (continued).

Solvent name	$\delta_D / \text{MPa}^{1/2}$	$\delta_P / \text{MPa}^{1/2}$	$\delta_H / \text{MPa}^{1/2}$	Radius	Status
Solketal	16.6	7.9	12.0	5.32	Pass
<i>t</i> -Butyl ethyl ether	14.4	3.5	2.7	10.5	Fail
Tetrahydrofuran	16.8	5.7	8.0	4.34	Pass
Tetrahydrofurfuryl alcohol	17.8	8.2	12.9	5.33	Pass

Triacetin	16.5	4.5	9.1	5.83	Pass
Triethyl citrate	16.5	4.9	12	6.84	Fail
α -Pinene	16.4	1.1	2.2	10.4	Fail
α -Terpineol	17.1	3.6	7.6	5.98	Pass
β -Pinene	16.3	1.1	1.9	10.6	Fail
γ -Valerolactone	16.9	11.5	6.3	3.41	Pass

Surface energy. Only eleven of the bio-based solvents pass the surface tension requirement, and 53 in total (Table S6). No surface tension data for γ -valerolactone was available, but considering its successful progress in other aspects of the solvent selection process it was important in this case to have an idea of its surface tension through computational estimates. Using HSPiP, the surface tension of γ -valerolactone was calculated to be unsatisfactory (29.9 mN m^{-1}). The same applies for dimethyl isosorbide. Experimental testing of these two promising solvents should be considered in future studies. Six bio-based solvents pass the requirements for both the polarity and the surface tension criteria: butyl lactate, Cyrene, furfural, levulinic acid, tetrahydrofurfuryl alcohol and triacetin.

Table S6. Surface tension characteristics of the bio-based solvents.

Solvent name	Surface tension $/\text{mN m}^{-1}$	Status
1,2-Pentanediol		No data
1,2-Propanediol	40.1	Pass
1,3-Propanediol		No data
1,4-Butanediol	44.6	Fail
1-Butanol	24.7	Fail

2-Butanol	23.4	Fail
2-Methyltetrahydrofuran		No data
2-Octanol	26.4	Fail
2-Propanol	20.9	Fail
Acetic acid	27.4	Fail
Acetone	22.7	Fail
Acetyltributyl citrate		No data
Butyl lactate	35.0	Pass
Butyric acid	26.7	Fail
Cyrene	33.6	Pass
Diethoxymethane	21.6	Fail
Dimethyl ether	16.0	Fail
Dimethyl isosorbide		(Fail)*
Dimethyl sulphoxide	43.0	Pass
<i>d</i> -Limonene	26.9	Fail

Table S6. Surface tension characteristics of the bio-based solvents. (continued).

Solvent name	Surface tension /mN m ⁻¹	Status
Ethanol	21.2	Fail
Ethyl acetate	23.8	Fail
Ethyl lactate	29.2	Fail
Ethylene glycol	48.5	Fail
Eugenol	30.9	Fail
Furfural	43.5	Pass

Furfuryl alcohol	38.0	Pass
Glycerol	63.4	Fail
Glycerol carbonate		No data
Glycerol formal	44.5	Fail
Isoamyl alcohol	23.8	Fail
Isobutanol	23.0	Fail
Isoeugenol	30.8	Fail
Lactic acid		No data
Lauric acid	26.6	Fail
Levulinic acid	39.7	Pass
Methanol	22.3	Fail
Methyl lactate	39.0	Pass
Methyl oleate	31.3	Fail
Oleic acid	32.8	Pass

Table S6. Surface tension characteristics of the bio-based solvents. (continued).

Solvent name	Surface tension /mN m⁻¹	Status
<i>p</i> -Cymene	28.1	Fail
Solketal	32.1	Fail
<i>t</i> -Butyl ethyl ether	19.1	Fail
Tetrahydrofuran	26.4	Fail
Tetrahydrofurfuryl alcohol	37.0	Pass
Triacetin	35.5	Pass
Triethyl citrate		No data

α -Pinene	25.9	Fail
α -Terpineol	31.6	Fail
β -Pinene	26.9	Fail
γ -Valerolactone		(Fail)*

*No experimental data was available. The calculated surface tension did not meet the requirement.

Viscosity. At this point it is worth emphasising that polarity (a thermodynamic trait) is not the only solvent property responsible for solubility. Kinetic factors are also applicable. The frictional forces present between solvent and solute, and the resulting settling velocity when establishing the suspension of graphene particles are likely to influence the concentration and stability of the dispersion. Although applied for spherical particles, we assume here that Stokes' law can also be used in this instance (*i.e.* for flat laminates).³³ According to Stokes' law, the settling velocity under centrifugation is given by equation 5:

$$V_s = \frac{8}{9} \frac{r_g^2 \pi^2 f^2 R (\rho_g - \rho_s)}{\mu} \quad \text{Eq. (5)}$$

Most of the variables relate to the particles, with r_g representing the lateral average size of graphene flakes; f is the number of rotations (which is 1167 s^{-1} in our experiments); R is the radius of the centrifuge (the distance of the bottom of the tube to the centre, in this case 8 cm); and ρ_g is the density of graphene.

The two solvent properties, and therefore the variables relevant in this solvent screening, are the solvent density ρ_s and dynamic viscosity μ . According to equation 5 the ratio of density to viscosity will therefore influence the settling velocity of particles in suspension. A small density/dynamic viscosity ratio is desirable in this instance (equivalent to

the inverse of kinematic viscosity). We have proposed that a low settling velocity caused by high kinematic viscosity contributes to a higher concentration of dispersed graphene after centrifugation because of the increased stability of the dispersion. Evidence that viscosity is also related to the quality of graphene has also been provided (refer to Raman spectroscopy experiments in the main article and the Experiment Results section of this Supporting Information).

An arbitrary upper limit to the density/viscosity ratio of $1.20 \text{ g mL}^{-1} \text{ cP}^{-1}$ was implemented so to contain the recognised solvents with known high performance (NMP, DMF, and 1,2-DCB) but exclude enough solvents to justify the exercise. This produced 127 candidates from 199 entries. This was calculated independently of whether the polarity and surface tension of each solvent candidate was deemed as suitable or not. Of the solvent candidates with an ideal density to viscosity ratio, many are plasticisers, diols, and other glycerol derivatives too polar to qualify as graphene processing solvents (at least using the conditions reported here). Most of the bio-based solvents pass this criterion of the assessment, with the exception of 2-methyltetrahydrofuran, acetone, ethyl acetate, methanol, and tetrahydrofuran, and 8 further solvents without viscosity data (Table S7).

Table S7. Viscosity characteristics of the bio-based solvents.

Solvent name	Density (ρ) /g mL ⁻¹	Viscosity (μ) /g s ⁻¹ m ⁻¹	ρ/μ	Status
1,2-Pentanediol				No data
1,2-Propanediol	1.04	56	0.019	Pass
1,3-Propanediol				No data
1,4-Butanediol	1.02	84.9	0.012	Pass
1-Butanol	0.81	2.5	0.32	Pass

2-Butanol	0.80	3.0	0.27	Pass
2-Methyltetrahydrofuran	0.85	0.46	1.9	Fail
2-Octanol	0.82	6.5	0.13	Pass
2-Propanol	0.79	2.0	0.39	Pass
Acetic acid	1.04	1.1	0.99	Pass
Acetone	0.79	0.32	2.5	Fail
Acetyltributyl citrate	1.05	42.7	0.025	Pass
Butyl lactate	0.98	3.8	0.26	Pass
Butyric acid	0.96	1.4	0.67	Pass
Cyrene	1.25	14.5	0.086	Pass
Diethoxymethane				No data

Table S7. Viscosity characteristics of the bio-based solvents. (continued).

Solvent name	Density (ρ) /g·mL ⁻¹	Viscosity (μ) /g·s ⁻¹ ·m ⁻¹	ρ/μ	Status
Dimethyl ether				No data
Dimethyl isosorbide	1.15	5	0.23	Pass
Dimethyl sulphoxide	1.10	2.0	0.55	Pass
<i>d</i> -Limonene	0.84	0.92	0.91	Pass
Ethanol	0.79	1.1	0.74	Pass
Ethyl acetate	0.89	0.44	2.0	Fail
Ethyl lactate	1.03	2.7	0.38	Pass
Ethylene glycol	1.11	16.1	0.069	Pass
Eugenol	1.07	7.8	0.14	Pass
Furfural	1.15	1.6	0.73	Pass
Furfuryl alcohol	1.13	4.6	0.24	Pass
Glycerol	1.25	954	0.0013	Pass
Glycerol carbonate	1.4	85	0.017	Pass

Glycerol formal	1.22	14.2	0.086	Pass
Isoamyl alcohol	0.81	4.2	0.19	Pass
Isobutanol	0.80	4.7	0.17	Pass
Isoeugenol	1.08	7.5	0.15	Pass
Lactic acid				No data
Lauric acid	0.87	7.3	0.12	Pass
Levulinic acid				No data
Methanol	0.79	0.54	1.5	Fail
Methyl lactate	1.09	2.9	0.38	Pass
Methyl oleate	0.87	4.9	0.18	Pass

Table S7. Viscosity characteristics of the bio-based solvents (continued).

Solvent name	Density (ρ) /g·mL ⁻¹	Viscosity (μ) /g·s ⁻¹ ·m ⁻¹	ρ/μ	Status
Oleic acid	0.89	25.6	0.035	Pass
<i>p</i> -Cymene				No data
Solketal	1.07	11	0.097	Pass
<i>t</i> -Butyl ethyl ether				No data
Tetrahydrofuran	0.89	0.53	1.7	Fail
Tetrahydrofurfuryl alcohol	1.05	6.2	0.17	Pass
Triacetin	1.16	17.4	0.066	Pass
Triethyl citrate	1.14	35.2	0.032	Pass
α -Pinene	0.86	1.3	0.67	Pass
α -Terpineol	0.94	36.5	0.026	Pass
β -Pinene	0.86	1.5	0.57	Pass
γ -Valerolactone	1.05	2.2	0.48	Pass

Environmental health and safety. At this juncture it is prudent to review the current status of the solvent candidates. In total 22 solvents have the required polarity, viscosity, and

surface tension characteristics, including the benchmark solvents NMP, DMF, and 1,2-dichlorobenzene (Table S8). Environmental, health and safety (EHS) criteria were applied to the remaining 22 solvents. Five bio-based solvents are contained within this set. Levulinic acid did not have sufficient data to complete the viscosity assessment, but has recently been reported elsewhere as a viable graphene processing solvent.³⁴

Table S8. Summary of solvent selection candidates.

Solvent	Polarity			Radius	Surface tension /mN.m ⁻¹	Viscosity /g·s ⁻¹ ·m ⁻¹
	δ _D	δ _P	δ _H			
1,1,2,2-Tetrachloroethane	18.8	5.1	5.3	5.1	34.7	1.8
1,2,3-Trichloropropane	17.8	12.3	3.4	5.3	37.7	2.5
1,2-Dichlorobenzene	19.2	6.3	3.3	5.8	36.6	1.3
Acetophenone	18.8	9.0	4.0	4.0	39.8	1.7
Aniline	20.1	5.8	11.2	6.5	41.1	4.4
Benzaldehyde	19.4	7.4	5.3	4.2	38	1.3
Benzonitrile	18.8	12	3.3	5.4	38.8	1.3
Butyl lactate	15.8	6.5	10.2	5.8	35	3.8
Cyclohexanone	17.8	8.4	5.1	2.8	35.1	2.2
Cyclopentanone	17.9	11.9	5.2	3.6	33.2	1.29
Cyrene	18.8	10.6	6.9	2.2	33.6	14.5
Diethyl phthalate	17.6	9.6	4.5	3.3	37.5	12.9
Diethylene glycol monobutyl ether	16.0	7.0	10.6	5.5	32.8	4.9
Furfural	18.6	14.9	5.1	6.3	43.5	1.6
Morpholine	18.0	4.9	11.0	5.5	37.5	2.2
DMAc	16.8	11.5	9.4	3.7	32.4	0.9
DMF	17.4	13.7	11.3	5.8	35	0.8
Nitrobenzene	20.0	10.6	3.1	6.2	43.4	1.8

NMP	18.0	12.3	7.2	3.0	40.7	1.7
Pyridine	19.0	8.8	5.9	2.7	36.6	0.9
Tetrahydrofurfuryl alcohol	17.8	8.2	12.9	5.3	37	6.2
Triacetin	16.5	4.5	9.1	5.8	35.5	17.4

As a first pass greenness assessment, the safety datasheet (obtained from Sigma-Aldrich) of each of the 22 shortlisted solvents was used to immediately rule out candidates based on their toxicity profile (Table S9). Any solvent that causes cancer in humans, has been found to be mutagenic, or is reprotoxic was rejected in line with REACH CMR requirements (Table S3). Entries in orange in Table S9 indicate likely chronic toxicity in humans based on animal studies. Solvents that are severely acutely toxic (*e.g.* represented by any of the hazard statements H300, H301, H310, H331, H330, H331 as defined in the CLP directive) were also removed from the final candidate list, leaving only eight solvents remaining. No solvent candidates of the 22 on the shortlist were classifiable as PBT, although the aquatic toxicity of several candidates is high (see supplementary spreadsheet file).

Table S9. Solvent toxicology data screening.

Solvent	Carcinogenicity	Mutagenicity	Reproductive toxicity	Acute toxicity
1,1,2,2-Tetrachloroethane				H310 & H330
1,2,3-Trichloropropane	Category 1B (H350)	Category 2 (H341)	Category 1B (H360)	H301 & H311 & H331
1,2-Dichlorobenzene	Pass			
Acetophenone		Positive animal tests		
Aniline	Category 2 (H351)	Category 2 (H341)		H301 & H311 & H331
Benzaldehyde		Positive animal tests		
Benzonitrile			Pass	
Butyl lactate			Pass	
Cyclohexanone			Pass	
Cyclopentanone			Pass	
Cyrene			Pass	
Diethyl phthalate			Positive animal tests	

Table S9. Solvent toxicology data screening. (continued).

Solvent	Carcinogenicity	Mutagenicity	Reproductive toxicity	Acute toxicity
Diethylene glycol monobutyl ether	REACH restriction already in place: “ <i>Shall not be placed on the market for supply to the general public, as a constituent of spray paints or spray cleaners in aerosol dispensers in concentrations equal to or greater than 3 % by weight</i> ” (EU regulation (EC) No 1907/2006).			
Furfural	Category 2 (H351)	Positive animal tests		H301 & H331
Morpholine		Positive animal tests		
<i>N,N</i> -Dimethylacetamide			Category 2 (H360D)	
DMF			Category 2 (H360D)	
Nitrobenzene	Category 1B (H351)		Category 1B (H360F)	H301 & H311 & H331
NMP			Category 2 (H360)	
Pyridine	Pass			
Tetrahydrofurfuryl alcohol			Category 1B (H360Df)	
Triacetin	Pass			

Greenness assessment. The final phase of the solvent selection process relates to the greenness of each remaining solvent. The greenness assessment was only applied to the eight solvent candidates fulfilling the earlier performance requirements and EHS requirements to reduce the data gathering exercise. Cyrene is the only wholly bio-based solvent remaining. Butyl lactate is partially bio-based at present, as is triacetin. The technology exists to produce

wholly bio-based butyl lactate and triacetin, but the price and availability of bio-1-butanol and bio-based acetic acid means for the time being their petrochemical equivalents are used to produce the downstream solvents. This was not seen as a concern in the long term, with the lower threshold for bio-based solvents set at 25% bio-based carbon content (Table S4). For the 5 other solvents (1,2-dichlorobenzene, benzonitrile, cyclohexanone, cyclopentanone, and pyridine) the lack of a commercially proven renewable feedstock for manufacture is disadvantageous.

Greenness criteria were selected in an attempted to cover the different aspects of the solvent life cycle while also being validated by regulations. This exercise is not intended to rule out any of the final eight solvent candidates, instead its purpose is to create a hierarchy within these remaining solvents.

Seven physical property and toxicology data sets were obtained and related to consequential environmental, health and safety effects. The criteria were vapour pressure (low values are ideal to reduce VOC losses into atmosphere), autoignition temperature and flash point (for safety considerations), and rat oral LD₅₀ (a health measure). In terms of environmental issues, lipophilicity (low logP values suggest a low potential for bioaccumulation) and aquatic toxicity were also considered in addition to biodegradability. Indicators for these criteria were presented earlier (Table S4). The greenness of the final eight solvent candidates can be compared to identify the most favourable options. A detailed examination is featured in the accompanying spreadsheet. For here it suffices to say that of the eight solvents, only triacetin is free of any breaches of legislated threshold values (Table S10). Butyl lactate and Cyrene are both VOCs. In addition to being VOCs, the five petrochemical solvents are all *harmful if swallowed* (whereas the bio-based solvents are not). Furthermore, 1,2-dichlorobenzene is hazardous to the aquatic environment, and cyclohexanone, cyclopentanone, and pyridine are all regarded as *flammable liquids* because

of their low flash points. For these reasons butyl lactate, Cyrene, and triacetin were employed as solvents in experimental graphene processing (Figure S12). The results are reported in the main article.

Table S10. Solvent greenness issues.

Solvent	Breaches of regulatory limits relating to solvent greenness
1,2-Dichlorobenzene	CLP 'acute toxicity' threshold (harmful if swallowed); Industrial emissions VOC definition; CLP 'harmful to the aquatic environment'.
Benzonitrile	CLP 'acute toxicity' threshold (harmful if swallowed); Industrial emissions VOC definition.
Butyl lactate	Industrial emissions VOC definition.
Cyclohexanone	CLP 'acute toxicity' threshold (harmful if swallowed); CLP 'flammable liquids' threshold; Industrial emissions VOC definition.
Cyclopentanone	CLP 'acute toxicity' threshold (harmful if swallowed); CLP 'flammable liquids' threshold; Industrial emissions VOC definition.
Cyrene	Industrial emissions VOC definition.
Pyridine	CLP 'acute toxicity' threshold (harmful if swallowed); CLP 'flammable liquids' threshold; Industrial emissions VOC definition.
Triacetin	None.

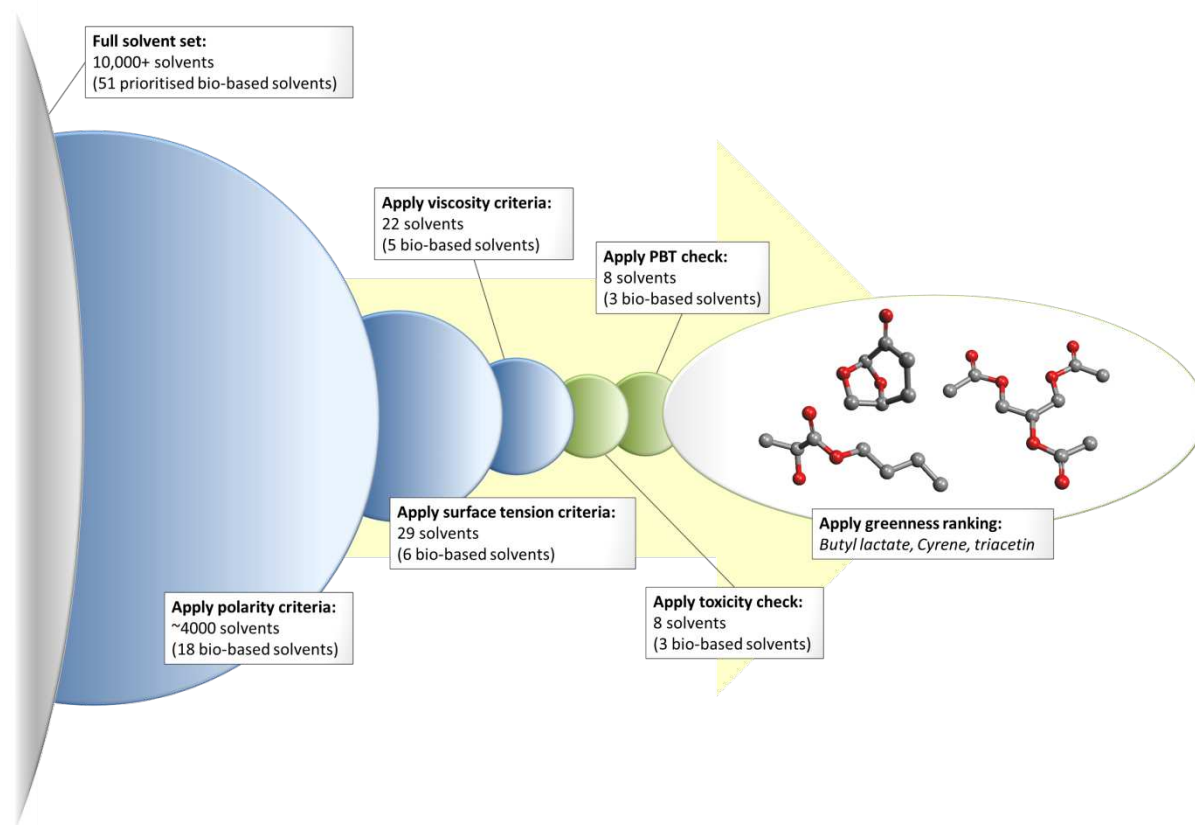


Figure S12. A schematic of the solvent selection process, refining a large dataset to three bio-based solvent candidates.

It should also be recognised that four of the solvents: benzonitrile, cyclohexanone, cyclopentanone, and pyridine, have been tested previously as graphene dispersion solvents,²⁶ and additionally 1,2-dichlorobenzene is an established solvent of course.³⁵ The prior existence of experimental data is useful to validate the solvent selection process, and can even be used to improve the protocol in subsequent reiterations. Of these solvents, cyclohexanone and cyclopentanone had previously been put forward as greener and more efficient graphene processing solvents.²⁹ Similarly benzonitrile also offered greater concentrations of graphene than NMP. In the same polarity relationship study pyridine was reported as a poor solvent,²⁶ which is unexpected from the conclusion of the solvent selection process in this work. One explanation could be the relatively low viscosity of pyridine for a graphene solvent, which is close to the cut-off threshold that was established in the solvent

selection process. Also note however that other reports show the successful use of pyridine as a graphene processing solvent,³⁶ and so the distinction between good and poor graphene processing solvents remains slightly elusive. That is why a multi-criteria solvent selection protocol was designed, and a number of solvent candidates shortlisted rather than only one.

Overview of advantages of Cyrene compared to NMP. Table S11 provides the numerical data given in Figure 1 of the main article.

Table S11. Relevant properties of Cyrene and NMP.

	Solvent properties	NMP	Cyrene
<i>Physical properties</i>	Density (ρ), g cm ⁻³	1.03	1.24
	Viscosity (μ), cP	1.7	10.5
	Surface tension (γ), mN m ⁻¹	40.7	33.6
	Surface energy (ϵ),* mN m ⁻¹	70.5	63.4
	Dispersive Hansen parameter (δ_D), [§] MPa ^{0.5}	18.0	18.8
	Polar Hansen parameter (δ_P), [§] MPa ^{0.5}	12.3	10.6
	Hydrogen bonding Hansen parameter (δ_H), [§] MPa ^{0.5}	7.2	6.9
<i>Environmental health and safety considerations</i>	Vapor pressure, mmHg	0.34	0.21
	Flash point (closed cup), °C	92	108
	Bio-based content	0%	100%
	logP	-0.38	-1.52

*Calculated according to the equation: $\gamma = \epsilon - TS$, where the surface entropy, S takes the same value for both solvents,³ of $S \sim 0.1 \text{ mJ m}^{-2} \text{ K}^{-1}$

[§]Calculated with HSPiP software.

References

1. Court, G. R.; Lawrence, C. H.; Raverty, W. D.; Duncan, A. J. Method for converting lignocellulosic materials into useful chemicals. World patent **2011**, WO 2011000030 A1.
2. Sherwood, J.; De bruyn, M.; Constantinou, A.; Moity, L.; McElroy, C. R.; Farmer, T. J.; Duncan, T.; Raverty, W.; Hunt, A. J.; Clark, J. H. Dihydrolevoglucosenone (Cyrene) as a bio-based alternative for dipolar aprotic solvents. *Chem. Commun.* **2014**, *50*, 9650-9652.
3. Hernandez, Y.; Nicolosi, V.; Lotya, M.; Blighe, F. M.; Sun, Z.; De, S.; McGovern, I. T.; Holland, B.; Byrne, M.; Gun'Ko, Y. K.; Boland, J. J.; Niraj, P.; Duesberg, G.; Krishnamurthy, S.; Goodhue, R.; Hutchison, J.; Scardaci, V.; Ferrari, A. C.; Coleman, J. N. High-yield production of graphene by liquid-phase exfoliation of graphite. *Nat. Nano.* **2008**, *3*, 563-568.
4. Graphenea. Graphenea Monolayer Graphene film - Product Datasheet. Available from:
http://cdn.shopify.com/s/files/1/0191/2296/files/Graphenea_Monolayer_Film_Datasheet_2014-03-25.pdf?2923 (accessed 21/10/2015).
5. Wang, S.; Zhang, Y.; Abidi, N.; Cabrales, L. Wettability and surface free energy of graphene films. *Langmuir* **2009**, *25*, 11078-11081.
6. Coleman, J. N. Liquid exfoliation of defect-free graphene. *Acc. Chem. Res.* **2013**, *46*, 14-22.
7. Rafiee, J.; Mi, X.; Gullapalli, H.; Thomas, A. V.; Yavari, F.; Shi, Y.; Ajayan, P. M.; Koratkar, N. A. Wetting transparency of graphene. *Nat. Mater.* **2012**, *11*, 217-222.

8. Taherian, F.; Marcon, V.; van der Vegt, N. F. A.; Leroy, F. What is the contact angle of water on graphene? *Langmuir* **2013**, *29*, 1457-1465.
9. Salavagione, H. J.; Martínez, G.; Ellis, G. Graphene-Based Polymer Nanocomposites. In *Physics And Applications Of Graphene - Experiments*. Mikhailov, S., Eds.; InTech: Vienna, 2011; pp 169-192.
10. Li, Z.; Wang, Y.; Kozbial, A.; Shenoy, G.; Zhou, F.; McGinley, R.; Ireland, P.; Morganstein, B.; Kunkel, A.; Surwad, S. P.; Li, L.; Liu, H. Effect of airborne contaminants on the wettability of supported graphene and graphite. *Nat. Mater.* **2013**, *12*, 925-931.
11. Li, X.; Cai, W.; An, J.; Kim, S.; Nah, J.; Yang, D.; Piner, R.; Velamakanni, A.; Jung, I.; Tutuc, E.; Banerjee, S. K.; Colombo, L.; Ruoff, R. S. Large-area synthesis of high-quality and uniform graphene films on copper foils. *Science* **2009**, *324*, 1312-1314.
12. Reina, A.; Jia, X.; Ho, J.; Nezich, D.; Son, H.; Bulovic, V.; Dresselhaus, M. S.; Kong, J. Large area, few-layer graphene films on arbitrary substrates by chemical vapor deposition. *Nano. Lett.* **2009**, *9*, 30-35.
13. Malard, L. M.; Pimenta, M. A.; Dresselhaus, G.; Dresselhaus, M. S. Raman spectroscopy in graphene. *Phys. Rep.* **2009**, *473*, 51-87.
14. Pimenta, M. A.; Dresselhaus, G.; Dresselhaus, M. S.; Cançado, L. G.; Jorio, A.; Saito, R. Studying disorder in graphite-based systems by Raman spectroscopy. *Phys. Chem. Chem. Phys.* **2007**, *9*, 1276-1290.
15. Ferrari, A. C. Raman spectroscopy of graphene and graphite: disorder, electron-phonon coupling, doping and nonadiabatic effects. *Solid State Commun.* **2007**, *143*, 47-57.

16. Hao, Y.; Wang, Y.; Wang, L.; Ni, Z.; Wang, Z.; Wang, R.; Koo, C. K.; Shen, Z.; Thong, J. T. L. Probing layer number and stacking order of few-layer graphene by Raman spectroscopy. *Small* **2010**, *6*, 195-200.
17. Cançado, L. G.; Takai, K.; Enoki, T.; Endo, M.; Kim, Y. A.; Mizusaki, H.; Jorio, A.; Coelho, L. N.; Magalhães-Paniago, R.; Pimenta, M. A. General equation for the determination of the crystallite size L_a of nanographite by Raman spectroscopy. *Appl. Phys. Lett.* **2006**, *88*, 163106.
18. Cançado, L. G.; Jorio, A.; Martins Ferreira, E. H.; Stavale, F.; Achete, C. A.; Capaz, R. B.; Moutinho, M. V. O.; Lombardo, A.; Kulmala, T. S.; Ferrari, A. C. Quantifying defects in graphene via Raman spectroscopy at different excitation energies. *Nano Lett.* **2011**, *11*, 3190-3196.
19. Khan, U.; O'Neill, A.; Lotya, M.; De, S.; Coleman, J. N. High-concentration solvent exfoliation of graphene. *Small* **2010**, *6*, 864-871.
20. Sun, Z.; Vivekananthan, J.; Guschin, D. A.; Huang, X.; Kuznetsov, V.; Ebbinghaus, P.; Sarfraz, A.; Muhler, M.; Schuhmann, W. High concentration graphene dispersions with minimal stabilizer: a scaffold for enzyme immobilization for glucose oxidation. *Chem. Eur. J.* **2014**, *20*, 5752-5761.
21. Gani, R.; Jiménez-González, C.; Constable, D. J. C. Method for selection of solvents for promotion of organic reactions. *Computers & Chemical Engineering* **2005**, *29*, 1661-1676.
22. O'Neill, A.; Khan, U.; Nirmalraj, P. N.; Boland, J.; Coleman, J. N. Graphene dispersion and exfoliation in low boiling point solvents. *J. Phys. Chem. C* **2011**, *115*, 5422-5428.

23. Cheng, Q.; Debnath, S.; Gregan, E.; Byrne, H. J. Ultrasound-assisted SWNTs dispersion: effects of sonication parameters and solvent properties. *J. Phys. Chem. C* **2010**, *114*, 8821-8827.
24. Yousefinejad, S.; Honarasa, F.; Abbasitabar, F.; Arianezhad, Z. New LSER model based on solvent empirical parameters for the prediction and description of the solubility of buckminsterfullerene in various solvents. *J. Solution Chem.* **2013**, *42*, 1620-1632.
25. Kim, J. H.; Lee, J. H. Preparation of graphite nanosheets by combining microwave irradiation and liquid-phase exfoliation. *J. Ceram. Process. Res.* **2014**, *15*, 341-346.
26. Hernandez, Y.; Lotya, M.; Rickard, D.; Bergin, S. D.; Coleman, J. N. Measurement of multicomponent solubility parameters for graphene facilitates solvent discovery. *Langmuir* **2010**, *26*, 3208-3213.
27. Yi, M.; Shen, Z. G.; Zhang, X. J.; Ma, S. L. Achieving concentrated graphene dispersions in water/acetone mixtures by the strategy of tailoring hansen solubility parameters. *J. Phys. D: Appl. Phys.* **2013**, *46*, 025301.
28. CEN/TS 16766:2015. *Bio-based solvents - Requirements and test methods*. CEN/TC 411 Bio-based products: European Committee for Standardization (2015).
29. Hansen, C. M. In *Hansen Solubility Parameters: A User's Handbook*; CRC press: Boca Raton, 2007.
30. Bergin, S. D.; Sun, Z.; Rickard, D.; Streich, P. V.; Hamilton, J. P.; Coleman, J. N. Multicomponent solubility parameters for single-walled carbon nanotube-solvent mixtures. *ACS Nano* **2009**, *3*, 2340-2350.
31. Shin, Y. J.; Wang, Y.; Huang, H.; Kalon, G.; Wee, A. T. S.; Shen, Z.; Bhatia, C. S.; Yang, H. Surface-energy engineering of graphene. *Langmuir* **2010**, *26*, 3798-3802.

32. Lim, H. J.; Lee, K.; Cho, Y. S.; Kim, Y. S.; Kim, T.; Park, C. R. Experimental consideration of the hansen solubility parameters of as-produced multi-walled carbon nanotubes by inverse gas chromatography. *Phys. Chem. Chem. Phys.* **2014**, *16*, 17466-17472.
33. Xiong, B.; Cheng, J.; Qiao, Y.; Zhou, R.; He, Y.; Yeung, E. S. Separation of nanorods by density gradient centrifugation. *J. Chromatogr. A* **2011**, *1218*, 3823-3829.
34. Sharma, M.; Mondal, D.; Singh, N.; Prasad, K. Biomass derived solvents for the scalable production of single layered graphene from graphite. *Chem. Comm.* **2016**. DOI: 10.1039/C6CC00256K.
35. Hamilton, C. E.; Lomeda, J. R.; Sun, Z.; Tour, J. M.; Barron, A. R. High-yield organic dispersions of unfunctionalized graphene. *Nano Lett.* **2009**, *9*, 3460-3462.
36. Park, K. H.; Kim, B. H.; Song, S. H.; Kwon, J.; Kong, B. S.; Kang, K.; Jeon, S. Exfoliation of non-oxidized graphene flakes for scalable conductive film. *Nano Lett.* **12**, 2871-2876 (2012).

Literature data (Note// this can be provided as a workable spreadsheet

Literature data for graphene dispersion solvents

Measurement of Multicomponent Solubility Parameters for Graphene Facilitates Solvent Discovery

Y. Hernandez, M. Lotya, D. Rickard, S. D. Bergin and J. N. Coleman, *Langmuir*, 2010, **26**, 3208-3213.

Solvent name	Concentration ($\mu\text{g}/\text{mL}$)	Relative concentration to NMP	Included on final solvent shortlist	Reasons for excluding high performance solvents in this assessment (see later)
Cyclopentanone	8,5	1,8	Yes	
Cyclohexanone	7,3	1,6	Yes	
N-Formyl piperidine	7,2	1,5		Lack of data.
Vinyl pyrrolidinone	5,5	1,2		Lack of data.
Dimethylimidazolidinone	5,4	1,1		Lack of data.
Bromobenzene	5,1	1,1		Failed density/viscosity requirement.
Benzonitrile	4,8	1,0	Yes	
Benzyl benzoate	4,7	1,0		Failed surface tension requirement.
NMP	4,7	1,0		Reprotoxic.
Dimethylpropylene urea	4,6	1,0		
γ -Butyrolactone	4,1	0,9		
DMF	4,1	0,9		
N-Ethyl pyrrolidinone	4,0	0,9		
Dimethyl acetamide	3,9	0,8		
Cyclohexyl pyrrolidinone	3,7	0,8		
DMSO	3,7	0,8		
Dibenzyl ether	3,5	0,7		
Chloroform	3,4	0,7		
2-Propanol	3,1	0,7		
Chlorobenzene	2,9	0,6		
N-Octyl pyrrolidinone	2,8	0,6		
1,3-Dioxolane	2,8	0,6		
Ethyl acetate	2,6	0,6		
Quinoline	2,6	0,6		
Benzaldehyde	2,5	0,5		
Ethanolamine	2,5	0,5		
Diethyl phthalate	2,2	0,5		
N-Decyl pyrrolidinone	2,1	0,4		
Pyridine	2,0	0,4	Yes	
Dimethyl phthalate	1,8	0,4		
Formamide	1,7	0,4		
Ethanol	1,6	0,3		
Vinyl acetate	1,5	0,3		
Acetone	1,2	0,3		
Water	1,1	0,2		
Ethylene glycol	1,0	0,2		
Toluene	0,8	0,2		
Heptane	0,3	0,1		
Hexane	0,2	0,04		
Pentane	0,2	0,03		

Literature conclusions for successful liquid exfoliation of graphite

Liquid Exfoliation of Defect-Free Graphene

J. N. Coleman, *Accounts of Chemical Research*, 2013, **46**, 14-22 (and references within).

Criteria

Surface energy	Solvents must have a surface energy similar to graphene to delaminate graphite:	$E / \text{mN m}^{-1}$ 68
Polarity	Solvents must have a certain polarity to successfully disperse graphene:	$\delta_D / \text{MPa}^{1/2}$ 18,0 $\delta_P / \text{MPa}^{1/2}$ 9,3 $\delta_H / \text{MPa}^{1/2}$ 7,7

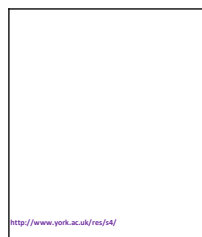
Problem definition

Method	Influential solvent parameters	Parameter 1					Parameter 2										
		Symbol	Value	Units	Description	Symbol	Value	Units	Description								
Stage	Description and identification of relevant solvent properties	Melting point	Boiling point	Vapour pressure	Density	Viscosity	Polarity	Surface tension	Partition coefficient	Water solubility							
1 Exfoliation	A mixture of the chosen solvent and graphite is treated with an ultrasonic probe. The solubility of graphene is dependent on the polarity and surface tension of the solvent. The effectiveness of the ultrasonic agitation is related to the viscosity and density of the solvent medium, but not in a way that is easily translated into target values for these properties given the present understanding of the process. See stage 2.	May effect sonication cavities					Stabilise exfoliated graphene										
2 Dispersion	The suspension is centrifuged and filtered. The stability of the graphene dispersion is influenced by the settling velocity of the particles, in turn dictated by the viscosity and density of the solvent.	Settling velocity (Stokes' law)					Density/viscosity										
3 Deposition	Samples were drop-casted for analysis (e.g. AFM) The solvent must be removable by evaporation in a controlled manner (80 °C under vacuum).	Rate of solvent removal					Boiling point										

The first phase of the solvent selection process is based on matching the physical properties of solvents to relevant requirements (target values and maximum or minimum permissible values). The relevant properties are highlighted in orange. Pale orange indicates a speculated effect. The requirements are then proposed. For example, polarity is defined with the Hansen solubility parameters. The target values are those of graphene. The flexibility of the assessment is limited to a certain radius when the distance between solute and solvent is plotted in the 3D Hansen space. The limits are set according to available solubility data. The target surface energy is that of graphene. The density and viscosity target is an arbitrary threshold.

This first phase of solvent selection (physical properties) has been developed in 3 stages. Stage 1 applies what is already understood in the literature. The results formed the initial evaluation of solvents in this work. This was expanded to include stage 2, which introduces the greater understanding we have developed in this work. Stage 3 is a proposal for future work, which will require some innovation to develop the necessary bespoke solvent systems that are viscous and volatile, and the correct polarity. After this first phase of solvent selection the toxicity and environmental impact of solvents is assessed in the context of regulation (phase 2), and finally the greenness of solvents was evaluated (phase 3).

Process	Worksheets
PHASE 1 Stage 1	"Polarity" "Surface tension"
PHASE 1 Stage 2	"Viscosity and density"
PHASE 1 Stage 3	Not attempted
PHASE 2 Stage 1	"Shortlist"
PHASE 2 Stage 2	"Shortlist"
PHASE 3	"Final decision"



Green Chemistry Review

Solvent selection stage gates

Phase 1		Phase 2		Phase 3	
Stage 1: Polarity and surface energy	Stage 2: Density and viscosity	Stage 3: Volatility (not applicable)	Stage 1: CMR, fatal acute toxicity	Stage 2: PBT (environmental impact)	Greenness
1,1,1,2-Tetrachloroethane	1,1,2,2-Tetrachloroethane				
1,2,3-Trichloropropane	1,2,3-Trichloropropane				
1,2-Dichlorobenzene	1,2-Dichlorobenzene		1,2-Dichlorobenzene	1,2-Dichlorobenzene	
1,2-Dichloroethane					
2-Pentanone					
Acetic anhydride					
Acetophenone	Acetophenone				
Aniline	Aniline				
Anisole					
Benzaldehyde	Benzaldehyde				
Benzonitrile	Benzonitrile		Benzonitrile	Benzonitrile	
Bromobenzene					
Butyl lactate	Butyl lactate		Butyl lactate	Butyl lactate	Butyl lactate
Cyclohexanone	Cyclohexanone		Cyclohexanone	Cyclohexanone	
Cyclopentanone	Cyclopentanone		Cyclopentanone	Cyclopentanone	
Cyrene	Cyrene		Cyrene	Cyrene	Cyrene
Diethyl phthalate	Diethyl phthalate				
Diethylene glycol monobutyl ether	Diethylene glycol monobutyl ether				
Furfural	Furfural				
Levulinic acid					
Morpholine	Morpholine				
N,N-Dimethyl acetamide	N,N-Dimethyl acetamide				
N,N-Dimethyl formamide	N,N-Dimethyl formamide				
Nitrobenzene	Nitrobenzene				
NMP	NMP				
Pyridine	Pyridine		Pyridine	Pyridine	
Tetrahydrofurfuryl alcohol	Tetrahydrofurfuryl alcohol				
Triacetin	Triacetin		Triacetin	Triacetin	Triacetin
Triethylphosphate					
29	22		8	8	3
6	5		3	3	3

Solvent name (3 demonstration examples)	Hansen D	Hansen P	Hansen H	Distance in Hansen space	Polarity
Toluene	18,0	1,4	2,0	9,74	FAIL
Acetone	15,5	10,4	7,0	5,17	PASS
Tetrahydrofuran	16,8	5,7	8,0	4,34	PASS

Polarity criteria key

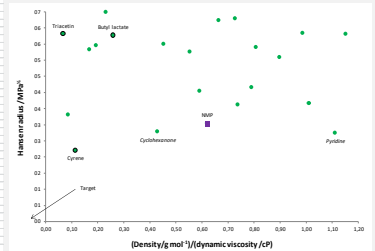
Distance <5	Pass
5 < Distance <6.5	Borderline (still considered a pass)
Distance >6.5	Fail

The full list of >10,000 solvents used in the polarity screening is not included in this spreadsheet for confidentiality reasons and conciseness. More than half were rejected because of their unsuitable polarity. Many of the remaining solvents are not realistically available to purchase, or do not have any physical property data meaning they cannot be included in subsequent assessments. A 'pass' is obtained when the distance in the Hansen space between solvent and solute is below 5.0 MPa^{0.5}. A borderline 'pass' is also awarded when this distance is between 5.0-6.5 MPa^{0.5} because some solvents that fall into this range are known to be good solvents (e.g. DMF) and others not (e.g. acetone). With several other factors responsible for the efficiency of graphene processing it is unclear at this stage where the ultimate solubility boundary is. **Solvents are presented in the "Shortlist" worksheet when data was available to assess at least one other criteria.** Note that all three of the solvents represented above failed both the viscosity and the surface tension criteria.

Target	Hansen D	Hansen P	Hansen H	Reference
Graphene	18,0	9,3	7,7	Hernandez <i>et al.</i> , <i>Langmuir</i> , 2010, 26 , 3208.

Shortlist

Subst name	Hansen D	Hansen P	Hansen H	Dielsmann H	Hansen spen	Polarity	Surface tension	Dielectric constant	All technical requirements	Polarity notes	Predictability (CMST) based on training	Final solvent candidate shortlist	Experimental concentration of expert and graph (relative to water)	References
------------	----------	----------	----------	-------------	-------------	----------	-----------------	---------------------	----------------------------	----------------	---	-----------------------------------	--	------------



Introducing density and viscosity as a combined parameter explains the poor performance of pyridine, and the high performance of cymene and cyclohexane. The density/viscosity threshold could have been optimized to each polymer, but we set what is a 1.5th DMF was accepted as having the correct physical properties. Butyl acetate and ethyl acetate are cymene as the focused solvents after passing phase 2 and phase 3 of the solvent selection procedure.

Final decision

This data has been extracted from the University of York 'Sol' solvent database. Values were collected from freely available sources except the Cyrene data, which was requested from F. Hoffmann-La Roche Ltd. We would like to thank F. Hoffmann-La Roche Ltd. for allowing us to use this data from the SDS they compiled.

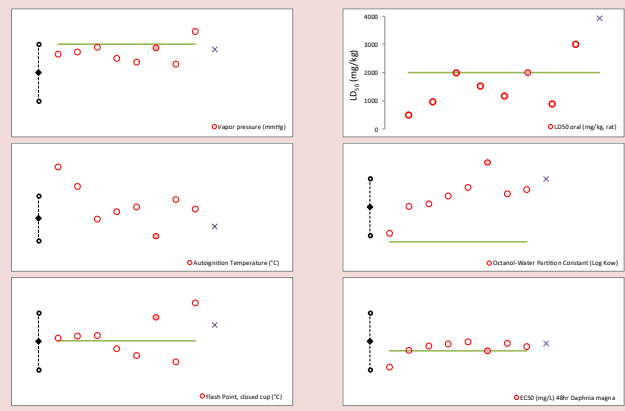
Solvent name	Bio-based carbon content (calculation)	Supplier	Autobiontem Temperature (°C)	Ref	Standard deviations from mean	Flash Point, closed cup (°C)	Ref	Standard deviations from mean	LD50 oral (mg/kg, rat)	log(LD50)	Test notes	Ref	Relative to LD50 of 2000 mg/kg	Vapor pressure (mmHg)	logVP	Temp. for vapor pressure (°C)	Ref	Standard deviations from mean (inserted as high values are desirable)	Octanol:Water Partition Constant (log Kow)	Ref	Standard deviations from mean (inserted as high values are desirable)	EC ₅₀ (mg/L) 48hr Daphnia magna	log(ES ₅₀)	Test notes	Ref	Standard deviations from mean	Biodegradation		
1,2-Dichlorobenzene	0%		548	MD5 (Sigma-Aldrich)	2.27	66	Rowen SGG	0.12	500	2.70		Rowen SGG	0.25	1.2E+00	0.08	20	MD5 (Sigma-Aldrich)	0.56	5.43	Rowen SGG	-0.54	0.74	-0.13	24hr	EPA ECTOX	-0.08	Considered biodegradable		
Benzonitrile	0%		550	MD5 (Sigma-Aldrich)	1.42	70	MD5 (Sigma-Aldrich)	0.19	971	2.99		MD5 (Sigma-Aldrich)	0.49	7.5E-01	-0.12	20	MD5 (Sigma-Aldrich)	0.72	3.56	MD5 (Sigma-Aldrich)	0.01	0.22	2.09	24hr	EPA ECTOX	-0.14	Considered biodegradable		
Butyl lactate	63%	Green Biologica	382	MSD	-0.05	71	SOLO-DB	0.21	2000	3.30		SOLO-DB	1.00	2.5E-01	-0.70	20	SOLO-DB	0.89	1.37	SOLO-DB	0.11	0.13	2.63		EPA ECTOX	-0.10	Considered biodegradable		
Cyclohexanone	0%		420	SOLO-DB	0.29	44	SOLO-DB	-0.26	1535	3.19		SOLO-DB	0.77	4.3E-01	0.64	25	SOLO-DB	0.49	0.81	ChemSpider	0.39	0.20	2.51	24hr	EPA ECTOX	-0.02	Considered biodegradable		
Cyclopentanone	0%		465	MD5 (Imperial College)	0.50	30	MD5 (Sigma-Aldrich)	-0.50	1180	3.07		MD5 (Sigma-Aldrich)	0.59	2.1E-01	1.08	25	MSD	0.37	0.24	(data sheet)	0.68	0.44	2.26	24 hr	EPA ECTOX	-0.26	Considered biodegradable		
Cyrene [®] Dihydrolevoglucosone	100%	Circo	296	F. Hoffmann-La Roche Ltd.	-0.80	108	F. Hoffmann-La Roche Ltd.	0.85	2000	3.30	min. value	F. Hoffmann-La Roche Ltd.	1.00	2.3E-01	-0.68	25	F. Hoffmann-La Roche Ltd.	0.88	-1.52	F. Hoffmann-La Roche Ltd.	1.58	3.00	2.00		F. Hoffmann-La Roche Ltd.	-0.17	Considered biodegradable		
Pyridine	0%		483	MD5 (Sigma-Aldrich)	0.83	37	MD5 (Sigma-Aldrich)	-0.79	801	2.95		MD5 (Sigma-Aldrich)	0.45	3.0E-01	1.30	25	MD5 (Sigma-Aldrich)	0.30	0.65	Rowen SGG	0.47	0.40	2.97		MD5 (Sigma-Aldrich)	-0.07	Considered biodegradable		
Hexan-2-one	33%	Reimsol	483	MD5 (Sigma-Aldrich)	0.40	138	MD5 (Sigma-Aldrich)	1.37	2000	3.48		MD5 (Sigma-Aldrich)	1.50	2.5E-01	-0.61	25	MD5 (Sigma-Aldrich)	0.45	0.58	MD5 (Sigma-Aldrich)	0.62	0.80	2.58		MD5 (Sigma-Aldrich)	-0.11	Considered biodegradable		
SA database mean average			387			59			5020	3.70				207		2.32		1.54		MD5 (Sigma-Aldrich)	0.47	1.00	1.26		MD5 (Sigma-Aldrich)	-0.11	Considered biodegradable		
SA database SD			135			68			2732	3.89				2497		1.65		1.87		MD5 (Sigma-Aldrich)	0.62	2.69	3.73		MD5 (Sigma-Aldrich)	-0.11	Considered biodegradable		
Mean + SD			502			117			759					3.55		1.71		3.55		MD5 (Sigma-Aldrich)	0.62	6.88			MD5 (Sigma-Aldrich)	-0.11	Considered biodegradable		
Mean - SD			279			1			-0.19					1.08				-0.39		MD5 (Sigma-Aldrich)	0.62	0.67			MD5 (Sigma-Aldrich)	-0.11	Considered biodegradable		
NMP (for comparison)	0%		386	MSD	-0.36	92	SOLO-DB	0.57	3914	3.59	SOLO-DB	1.00		3.4E-01	-0.47	25	SOLO-DB	0.87	0.38	ChemSpider	1.00	1.00	1.00	min. value 24hr	MD5 (Sigma-Aldrich)	-0.08	Considered biodegradable		
Regulatory limits and requirements in European standards	25% European standard 15/14766	n/a				66	CLP "flammable liquids" threshold	0.02	2000	3.30			CLP "acute toxicity" threshold	1.00	0.075	-1.12			Industrial Emissions 2010/75/EU "VOC" threshold	1.01		4	CLP "harmful to the aquatic environment" threshold (in practice EC 08-c100-010)	-1.23	100	2.00	CLP "harmful to the aquatic environment" threshold (in practice EC 08-c100-010)	-0.34	

Solvent name	# Best in class	# Worst in class	Bio-based?	Summation of scores	Rank	All breaches of regulatory limits
1,2-Dichlorobenzene	1	3	No	3.7	8	CLP "acute toxicity" threshold (harmful if swallowed); Industrial emissions VOC definition; CLP "harmful to the aquatic environment".
Benzonitrile			No	2.8	4	CLP "acute toxicity" threshold (harmful if swallowed); Industrial emissions VOC definition.
Butyl lactate			Partially	3.5	3	CLP "acute toxicity" threshold (harmful if swallowed); Industrial emissions VOC definition.
Cyclohexanone			No	3.6	5	CLP "acute toxicity" threshold (harmful if swallowed); CLP "flammable liquids" threshold; Industrial emissions VOC definition.
Cyclopentanone	1	1	No	2.5	6	CLP "acute toxicity" threshold (harmful if swallowed); CLP "flammable liquids" threshold; Industrial emissions VOC definition.
Cyrene [®] Dihydrolevoglucosone	1	1	Yes	3.5	2	Industrial emissions VOC definition.
Pyridine		2	No	2.2	7	CLP "acute toxicity" threshold (harmful if swallowed); CLP "flammable liquids" threshold; Industrial emissions VOC definition.
Hexan-2-one	3	1	Partially	4.8	1	None.
Triethylamine						

Summation of scores and the rank is purely for guidance.



Solvent data plotted against a scale of 0-4 (standard deviation (mean average shown as a black diamond); no deviation is made for LD₅₀, which is linear scale to give for improved clarity; solvent data shown as red circles (in the order left to right as listed in the table above); Cyrene is shown as a filled red data point; NMP (for reference) is given as a x data point, but please note NMP is reproductive, whereas the other solvents are not recognised as such; Regulation thresholds are given as a green line; high values indicate greener).



Bio-based solvent summary

Solvent name	Bio-based carbon content	Source	Supplier	Reference	Hansen D	Hansen P	Hansen H	Distance in Hansen space	Polarity	Surface tension	Density: viscosity	Additional comments
1,2-Pentanediol	100%	Pyrolysis of carbohydrate	Pennakem	agriobase.com/en/Database/BioProducts/Agriculture/forestry/culture/12-pentandiol (accessed 30-10-2015)	16.7	7.2	16.8	9.7	FAIL	NO DATA	NO DATA	
1,2-Propanediol	100%	Derived from glycerol	OnGen	agriobase.com/en/Database/BioProducts/food-and-drink/ethanol-4713-bio-propylene-glycol (accessed 30-10-2015)	15.8	10.4	21.3	13.8	FAIL	PASS	PASS	
1,3-Dioxolane-4-methanol (glycerol formal)	75%	Derived from glycerol	Lambiotte&Cie	agriobase.com/en/Database/BioProducts/Agriculture/forestry/culture/glycerol-formal (accessed 30-10-2015)	18.4	10.6	16.5	8.9	FAIL	FAIL	PASS	
1,3-Propanediol	100%	Derived from glycerol	DuPont-Tate & Lyle	agriobase.com/en/Database/BioProducts/Agriculture/forestry/culture/13-propanediol-biobased (accessed 30-10-2015)	16.8	13.5	23.2	16.2	FAIL	NO DATA	NO DATA	
1,4-Butanediol	100%	Fermentation product	Gemomatica	www.gemomatica.com/products/gemodaprocess (accessed 30-10-2015)	16.6	11	20.9	13.6	FAIL	FAIL	PASS	
1-Butanol	100%	Fermentation product (fuel market)	Numerous (fuel market)	www.bioinfo1.eurholland.com (accessed 30-10-2015)	16	5.7	15.8	9.7	FAIL	FAIL	PASS	
2-Butanol	100%	Fermentation product	DuPont	US patent 2008/0274525 A1	15.8	5.7	14.5	8.9	FAIL	FAIL	PASS	
2-Methyltetrahydrofuran	100%	Pyrolysis of carbohydrate	Pennakem	V. Pace et al., ChemSusChem., 2012, 5, 1369-1376.	16.9	5	4.3	5.9	PASS	NO DATA	FAIL	
2-Octanol	100%	Synthesised from vegetable oils	Arikama	agriobase.com/en/Database/BioProducts/chemistry/formulation-synthesis/2-octanol (accessed 30-10-2015)	16.1	4.2	9.1	6.5	FAIL	FAIL	PASS	
2-Propanol	100%	Fermentation product	Lanatzsch	US patent 2012/0521083 A1	15.8	6.1	16.4	10.3	FAIL	FAIL	PASS	
Acetic acid	100%	Fermentation product	Sekab	www.sekab.com/chemistry/acetic-acid (accessed 30-10-2015)	14.5	8	13.5	9.2	FAIL	FAIL	PASS	
Acetone	100%	Fermentation product	Numerous (plasticiser market)		15.5	10.4	7	5.2	PASS	FAIL	FAIL	
Acetyltributyl citrate	18%	Made from citric acid	Numerous (plasticiser market)		16.7	2.5	7.4	7.3	FAIL	NO DATA	PASS	
Butyl lactate	43-100%	Made from lactic acid	Galactec	www.lactec.com/en-us/products/productrange/plaster/K2784A2/galactec/K2784A2.aspx (accessed 30-10-2015)	15.8	6.5	10.2	5.8	PASS	PASS	PASS	Considered as a candidate
Butyric acid	100%	Fermentation product	Numerous (food and fragrances)		15.7	4.8	12	7.7	FAIL	FAIL	PASS	
Cyrene	100%	Pyrolysis of carbohydrate	Circa	J. Sherwood et al., Chem. Commun., 2014, 50, 9650-9652.	18.8	10.6	6.9	2.2	PASS	PASS	PASS	Considered as a candidate
Dioxolymethane (ethylal)	80%	Made with bio-ethanol	Lambiotte&Cie	agriobase.com/en/Database/BioProducts/chemistry/formulation-synthesis/ethylal (accessed 30-10-2015)	15.4	5.7	5.1	6.8	FAIL	FAIL	NO DATA	
Dimethyl ether	100%	Made from bio-gas	Chemrec	www.bioinfo1.eurholland.com (accessed 30-10-2015)	15.2	6.1	5.7	6.8	FAIL	FAIL	NO DATA	
Dimethyl isosorbide	75%	Pyrolysis of carbohydrate	Roquette and downstream	www.lorincrar.com/dimethyl-isosorbide-dm.html (accessed 30-10-2015)	17.6	7.1	7.5	2.4	PASS	FAIL*	PASS	*Based on predicted data from HSP17 (28.0 dynes/cm)
Dimethyl sulphoxide	100%	Made from dimethyl sulphide	Numerous (paper and pulp sector)		18.4	16.4	10.2	7.6	FAIL	PASS	PASS	
l-limonene	100%	Essential oils	Numerous (fragrance sector)	www.who.int/pqs/publications/cica/en/cica05.pdf (accessed 30-10-15)	17.2	1.8	4.3	8.4	FAIL	FAIL	PASS	
Ethanol	100%	Fermentation product	Numerous (fuel market)	www.bioinfo1.eurholland.com (accessed 30-10-15)	15.8	8.8	19.4	12.5	FAIL	FAIL	PASS	
Ethyl acetate	100%	Made from bio-ethanol	Sekab	www.sekab.com/chemistry/ethyl-acetate (accessed 30-10-2015)	15.8	5.3	7.2	6.0	PASS	FAIL	FAIL	
Ethyl lactate	100%	Made from lactic acid	Galactec		16	7.6	12.5	6.5	PASS	FAIL	PASS	
Ethylene glycol	100%	Made from bio-ethanol	India glycols	www.indiaglycols.com/product_group/monomethylene_glycol.htm (accessed 02-11-2015)	17	11	26	18.5	FAIL	FAIL	PASS	
Eugenol	100%	Essential oils	Numerous (fragrance sector)		19	7.5	13	5.9	PASS	FAIL	PASS	
Furfural	100%	Pyrolysis of carbohydrate	Numerous	www.furan.com/furfural.html (accessed 30-10-2015)	18.6	14.9	5.1	6.3	PASS	PASS	PASS	Eliminated on the basis of toxicity and mutagenicity
Furfuryl alcohol	100%	Pyrolysis of carbohydrate	Numerous	www.furan.com/furfuryl_alcohol_applications.html (accessed 02-11-2015)	17.4	7.6	15.1	7.7	FAIL	PASS	PASS	
Glycerol	100%	Vegetable oils	Numerous (fuel market)	V. Gal et al., Green Chem., 2010, 12, 1172-1178.	17.4	11.3	27.2	13.6	FAIL	PASS	PASS	
Glycerol carbonate	75%	Derived from glycerol	Glaucocemie	www.glaucocemie.de (accessed 02-11-2015)	17.9	25.5	17.4	18.9	FAIL	NO DATA	FAIL	
Isoamyl alcohol	100%	Fermentation product	Numerous (fuel oil)	US patent 2011,0087000 A1	15.8	5.2	13.3	8.2	FAIL	FAIL	PASS	
Isobutanol	100%	Fermentation product	Gevo		15.1	5.7	15.9	10.7	FAIL	FAIL	PASS	
Isosugonol	100%	Essential oils	Numerous (fragrance sector)		18.9	5.7	9.9	4.6	PASS	FAIL	PASS	
Lactic acid	100%	Fermentation product	Numerous (polymer market)	cellulac.co.uk/en/main/inputs-process-diagram (accessed 30-10-2015)	17.3	10.1	23.3	15.7	FAIL	NO DATA	NO DATA	
Lauric acid	100%	Vegetable oils	Numerous (fuel market)		16.2	4.1	7.4	6.3	PASS	FAIL	PASS	
Levulinic acid	100%	Pyrolysis of carbohydrate	GF Biochemicals	http://www.gfbiocemicals.com/products/Mevulinicacid	17.1	10.4	13.5	6.2	PASS	PASS	NO DATA**	**Viscosity data unavailable. Lower performance than NMP (see M. Sharma et al., Chem. Commun., 2016, DOI: 10.1039/C6CC02056K).
Methanol	100%	Made from bio-gas	Numerous	www.irena.org/DocumentDownloads/Publications/IRENA-ETSAP120Tech208IeR12008N20Production_of_Bio-methanol.pdf (accessed 02-11-2015)	14.7	12.3	22.3	16.3	FAIL	FAIL	FAIL	
Methyl lactate	75%	Made from lactic acid	Numerous (fuel market)		16.9	8.3	16.1	9.7	FAIL	PASS	PASS	
Methyl oleate	95%	Synthesised from vegetable oils	Numerous (fragrance sector)		16.2	3.8	4.5	7.3	FAIL	FAIL	PASS	
Oleic acid	100%	Vegetable oils	Numerous (fuel market)		16	2.8	6.2	7.8	FAIL	PASS	PASS	
p-Cymene	100%	Made from limonene/pinene	Numerous (fragrance sector)	J. A. Davis et al., Waste and Biomass Valorization, 2015, 6, 253-261.	17.3	2.4	2.4	8.8	FAIL	FAIL	NO DATA	
Solvent ((2,2-dimethyl-1,3-dioxolan-4-yl)methanol)(4-methanol)	50%	Derived from glycerol	Rhosia	www.rhosia.com/en/bio-based/Pתר_אגודות/12n.pdf (accessed 30-10-2015)	16.6	7.9	12.0	5.9	PASS	FAIL	PASS	
t-Butyl ethyl ether	33%	Made with bio-ethanol	Braskem	www.braskem.com/site.aspx?ethy-tertiary-butyl-ether (accessed 30-10-15)	14.4	3.5	2.7	10.5	FAIL	FAIL	NO DATA	
Tetrahydrofuran	100%	Pyrolysis of carbohydrate	Pennakem	agriobase.com/en/Database/BioProducts/chemistry/formulation-synthesis/THF (accessed 30-10-2015)	16.8	5.7	8	4.3	PASS	FAIL	FAIL	
Tetrahydrofurfuryl alcohol	100%	Pyrolysis of carbohydrate	Pennakem	agriobase.com/en/Database/BioProducts/Agriculture/forestry/culture/THF (accessed 30-10-2015)	17.8	8.2	12.9	6.3	PASS	PASS	PASS	
Triacetin	33%-100%	Derived from glycerol	Eastman	www.eastman.com/Products/Pages/ProductHome.aspx?Product=11051049 (accessed 30-10-2015)	16.5	4.5	9.1	5.8	PASS	PASS	PASS	Eliminated on the basis of reproductive toxicity
Triethyl citrate	100%	Made from citric acid	Numerous (plasticiser market)		16.5	4.9	12	6.8	FAIL	NO DATA	PASS	
α-Pinene	100%	Essential oils	Numerous (fragrance sector)		16.4	1.1	2.2	10.4	FAIL	FAIL	PASS	
α-Terpinolene	100%	Essential oils	Numerous (fragrance sector)		17.1	3.6	7.6	6.0	PASS	FAIL	PASS	
β-Pinene	200%	Essential oils	Numerous (fragrance sector)		16.3	1.1	1.9	10.6	FAIL	FAIL	PASS	
γ-Valerolactone	100%	Pyrolysis of carbohydrate	Numerous (fragrance/fuel additive)	http://www.adv-bio.com/ProductDetail.aspx?prodNo=1252	16.9	11.5	6.3	3.4	PASS	FAIL*	PASS	*Based on predicted data from HSP17 (29.9 dynes/cm). Failed as a solvent (see M. Sharma et al., Chem. Commun., 2016, DOI: 10.1039/C6CC02056K).

Total bio-based solvents considered: 51

18 11 80

